LBNL-55643 **TOPICAL REVIEW**

Cold Dark Matter and the LHC‡

Marco Battaglia[1,2]**, Ian Hinchliffe**[2]**, Daniel Tovey**[3]

[1]University of California, Dept. of Physics, Berkeley, CA
[2]Lawrence Berkeley National Laboratory, Berkeley, CA
[3]University of Sheffield, Dept. of Physics and Astronomy, Hounsfield Road, Sheffield, S3 7RH, UK

Abstract. The recent determination of the dark matter density in the Universe by the WMAP satellite has brought new attention to the interplay of results from particle physics experiments at accelerators and from cosmology. In this paper we discuss the prospects for finding direct evidence for a candidate dark matter particle at the LHC and the measurements which would be crucial for testing its compatibility with cosmology data.

1. Introduction

Recent precision data on the Cosmic Microwave Background (CMB) and other astrophysical measurements have confirmed that a substantial fraction of the mass of the universe is in the form of dark matter; that is matter which which cannot be observed directly using conventional astrophysical techniques. The COBE [1] satellite provided evidence for intrinsic anisotropies in the CMB spectrum. The superior resolution of the Wilkinson Microwave Anisotropy Probe (WMAP) mission has enabled the accurate extraction of the baryonic and dark matter densities of the universe. This has confirmed that the dark matter density exceeds that of baryonic matter in the universe by a factor of six [2]. The mass density is expressed as a fraction (referred to as Ω) of the amount required for an asymptotically flat universe and it is presently known to an accuracy of 7 %. The CMB results agree well with data obtained from supernovae and the rotation curves of spiral galaxies.

Dark matter, as opposed to dark energy, can exist in two forms: non-luminous baryonic matter in the form of large planets or dead stars (MACHOS), or weakly interacting elementary particles that pervade large regions of space. Searches for MACHOS have concluded that these cannot be responsible for a substantial part of the dark matter [3].

Particle physics candidates for dark matter fall into three basic categories depending upon their masses and interactions. Weakly interacting particles that are in thermal equilibrium at a very early stage in the evolution of the universe will eventually fall out of equilibrium as the universe expands. The decoupling time (or temperature) when this occurs depends on the expansion rate of the universe as well as the couplings of these particles to other particles that are still in equilibrium. Particles that are (non-)relativistic at the time that galaxies start to

‡ This work was supported in part by the Director, Office of Energy Research, Division of High Energy Physics of the U.S. Department of Energy under Contract DE-AC03-76SF00098

form are referred to as (cold) hot dark matter. The simplest example of hot dark matter is a neutrino with a very small mass ($< O(20)$ eV) and of cold dark matter a very heavy neutrino ($\sim$ 100 GeV). In both cases the interaction rates are determined by the Standard Model of electroweak interactions (SM).

The third type of particle dark matter can arise during the QCD phase transition as the universe cools down. In this case the result can be a gas of axions [4]. For certain values of the mass and coupling, these could account for a substantial part of the dark matter [5].

Hot and cold dark matter have implications for the distribution of visible matter (galaxies) throughout the universe [6]. The observed non-uniform distribution of such matter is believed to arise from the growth of quantum fluctuations remaining in the early universe after the end of inflation. These fluctuations are amplified by gravitational interactions and lead to the clumping that we observe today. The dark matter plays a vital role in this process as it dominates the total matter. Hot dark matter is free streaming and produces a universe with too little small scale structure. Cold dark matter is therefore strongly favored [2].

There are models of particle physics that provide natural candidates for relic particles comprising the cold dark matter. This article will discuss these candidates and how they could be produced and their properties inferred from experiments at the LHC. We shall comment on the interplay between the LHC experiments and terrestrial experiments that aim to detect the dark matter directly. Most of our discussion focuses on supersymmetric candidates.

Many of the candidate dark matter particles can be produced copiously at the LHC either directly or as decay products of the other particles. Measurements at the LHC will then provide information regarding the masses and couplings of both the dark matter candidate and the other particles with which it interacts and which are important in calculating its "relic" density.

In section 2.1 we review methodology by which the relic density is computed and discuss how the dark matter density constrains the possible supersymmetric models. We then discuss the constrained MSSM (CMSSM) model for which most of the detailed simulations have been carried out. The consequences of relaxing some of the CMSSM constraints are then discussed. This section concludes with a discussion of dark matter candidates in gauge and anomaly mediated models and of the possibility that sneutrinos or gluinos could account for the dark matter. Section 3 then discusses the potentially relevant LHC measurements of supersymmetric particles. The possibility that particles arising from models of extra dimensions could account for dark matter is discussed in Section 4. Section 5 then summarizes the constraints that can be obtained from direct searches for dark matter. In section 6 we illustrate how the measurements from LHC, astrophysics and direct detection complement each other and can be used to build up a complete picture of supersymmetric dark matter.

2. Cold Dark Matter and Supersymmetry

2.1. Supersymmetric Models

Supersymmetry (SUSY) is a symmetry which relates fermions and bosons. In supersymmetric theories all existing particles are accompanied by partners having opposite spin-statistics. It is an appealing concept, for which there is currently no direct experimental evidence. As none of the partner particles have been observed, supersymmetry cannot be exact and must be broken so that the masses of the superpartners are larger than a few hundred GeV [7]. Supersymmetry solves a long-standing problem with the SM, namely that the electroweak scale ($\sim$ the mass of the Z and W bosons) is of order 100 GeV even though radiative corrections in the model point to a scale that is many orders of magnitude larger, around the Planck scale (10^{19} GeV) where gravity becomes strong. A supersymmetric version of the SM is able to stabilize these radiative corrections and solve this "hierarchy problem" provided that the new particles have masses of less than a few TeV.

When supersymmetric models of electroweak interactions are constructed, there often arises a symmetry, called R-parity, under which all the existing particles are even and the new super-partners are odd. If R-parity is violated then supersymmetric models can naturally give rise to unacceptably short nucleon lifetimes. If R-parity is conserved, there are two important consequences; the supersymmetric particles have to be produced in pairs and the lightest of them is absolutely stable. In supersymmetric models the Lightest Supersymmetric Particle (LSP) is invariably produced abundantly in the early universe and hence if R-parity is conserved these LSPs should still be present throughout the universe, providing a natural candidate for the dark matter.

There are several candidates for the LSP, although many possibilities are ruled out by rather general considerations. Most importantly the LSP cannot carry electric charge as otherwise it would bind to ordinary matter, violating the very stringent limits which exist on exotic matter [8]. Remaining candidates are therefore the gravitino (partner of the graviton), $\tilde{G}$, the sneutrino (partner of the neutrino), $\tilde{\nu}$, the gluino (partner of the gluon), $\tilde{g}$, and the lightest neutralino, $\tilde{\chi}_1^0$, which is a mixture of the parters of the SM gauge bosons Z^0 and γ and the Higgs boson. In this last case, the coupling of the LSP is determined by its content. It is most convenient to work in a basis where the content is regarded as Higgsino, wino and bino, the neutral fermion states of the supersymmetric Higgs sector and the $SU(2)$ and $U(1)$ supersymmetric gauge theories. The first component couples like a Higgs boson and therefore has very weak couplings to quarks and leptons of the first two generations. The second component couples more strongly than the third due to the greater $SU(2)$ gauge coupling strength.

The simplest SUSY model, known as the "Minimal Supersymmetric Standard Model" or MSSM, is that containing one SUSY partner for each of the known SM particles together with two Higgs doublets to generate the masses of all the quarks and leptons. This model has over 100 parameters which control the masses and couplings of the new supersymmetric particles. These are determined by the mechanism responsible for SUSY breaking in the MSSM. There

are several candidates for the breaking mechanism which produce qualitatively different mass spectra. In general it is assumed that there is an additional "hidden" sector of the theory with particles of very large mass where SUSY exists as a broken symmetry. This breaking is communicated to the partners of the SM particles via a mediation mechanism.

Since gravity is known to exist, it is a natural candidate for the SUSY breaking mechanism and since it couples to all particles equally it is expected that all the sleptons, sneutrinos (partners of the charged leptons and neutrinos) and squarks (partners of quarks) will have a common mass at the energy scale where the mediation operates. Now the three couplings of the SM (the strong, weak and electromagnetic couplings) are precisely measured in current experiments, as are their evolutions with energy. If these couplings are extrapolated to very high energy assuming the existence of only the SM particles and their SUSY partners (with masses around 1 TeV) then it is found that they unify to a common value at a scale slightly below the Planck scale. This coincidence can be explained by postulating that the strong, weak and electromagnetic interactions are unified at this scale giving equal gluino and gaugino masses. These ideas are implemented in the SUGRA or constrained MSSM (CMSSM) model [9]. This has a total of five parameters: the common scalar mass m_0, which determines the squark, slepton, sneutrino and Higgs masses, the common gaugino mass $m_{1/2}$, which determines the gaugino and gluino masses, $\tan\beta$ which controls the relative size of the couplings of the Higgs boson to up and down type quarks, the sign of the Higgsino mass parameter μ, and the common trilinear coupling A_0, whose value is relevant only in a few cases. It is a remarkable feature of this model that, as the parameters are evolved down to lower energies, the masses change in a calculable way and, due to the large coupling of the top quark to the Higgs, electroweak symmetry is broken spontaneously and masses for the $W^{\pm}$ and Z^0 bosons generated automatically. As this model is simple, and fully described by a small number of parameters, it has been used most often for detailed phenomenological studies. Other models of SUSY breaking have different structures and we will comment on these later.

2.2. Computing the Cold Dark Matter Density

The maintenance of thermal equilibrium of particle densities in the early universe depends upon the interaction rates of the particles and the expansion rate of the universe. At very early times when the universe is at a very high temperature, all particles are in thermal equilibrium. Consider a particle that can annihilate against its anti-particle with a cross-section σ. The products of this annihilation are other (lighter) particles. The production and annihilation of the particles maintains their equilibrium. The time evolution of the number density n is described by:

$$\frac{dn}{dt} = -3Hn - <\sigma v>(n^2 - n_{eq}^2) \quad (1)$$

The first term on the right represents the dilution caused by the expansion of the universe, with H being the Hubble constant. The second term represents the effect of the annihilation, with v being the velocity of the particles and $<\sigma v>$ representing a thermal average of the cross-

section times velocity. n_{eq} is the number density at thermal equilibrium given by a Boltzmann distribution. If σ is sufficiently large, the second term ensures that $n = n_{eq}$, and hence the relic density is exponentially suppressed at temperatures where the particles are non-relativistic. If σ is very small then the particles cannot remain in equilibrium. For most processes interactions at sufficiently early time, or equivalently high temperature, are dominant, and equilibrium is maintained until the temperature falls below a freeze out temperature (T_F) when the interaction rate becomes too low and annihilation ceases. The number density at the present day is then given by $n_{eq}(T_F)$ diluted by the Hubble expansion. The surviving number is most sensitive to σ; a larger σ ensures a lower number of survivors and a smaller contribution to the mass density Ω. As the particle's mass increases its contribution to Ω also increases and therefore σ must be raised to satisfy experimental constraints. We shall frequently refer to this contribution to Ω arising from a specific dark matter particle as $\Omega_\chi h^2$, where the normalisation is appropriate for comparison with CMB data.

Amazingly, if supersymmetric particles have masses of order 100 GeV as indicated by the fine tuning argument discussed above, their present abundance is of the right magnitude to account for the "observed" cold dark matter. It is this fact that has led to such a large focus on supersymmetric dark matter candidates. In practice, the computation of the relic density of LSPs is more complicated than indicated above. There can be several supersymmetric particles with comparable masses, all of which are falling out of thermal equilibrium at the same time. As well as particle-anti-particle annihilation, processes involving the scattering of different species are important ("co-annihilation").

Several software packages have been developed to compute the cold dark matter density in a supersymmetric model with conserved R-parity [10, 11]. It is important to emphasize that the masses and couplings of the supersymmetric particles must be known before a prediction of the relic density can be obtained. Renormalization group equations (RGEs) are used to evolve the high scale CMSSM parameters and determine the soft parameters (masses and couplings) at the electroweak scale. Even small differences in these masses and couplings can result in significant changes in the predicted relic density. A recent survey found that the uncertainties in the masses of SUSY particles, defined by the differences between predictions from four independent programs, can be of order 20-30 % [12]. Both `DarkSusy` [11] `v. 4.0` and `micrOMEGAs` [10] `v. 1.3` can be interfaced to several different codes for computing the full SUSY spectrum including `ISASUSY` [13] and `SUSPECT` [14].

The main quantities which affect the relic density are the mass of the LSP and its interactions, determined by its composition. Over much of the CMSSM parameter space the LSP is the lightest neutralino, which usually consists predominantly of the partner of the gauge boson of the $U(1)$ sector of the SM (the bino). The coupling constant of this is the smallest of the three SM couplings and the annihilation cross-section is therefore small. The dominant mechanism contributing to σ is often $\tilde{\chi}_1^0\tilde{\chi}_1^0 \to \ell^+\ell^-$ which includes slepton exchange and is sensitive to the mass of the lightest slepton. In the CMSSM therefore, as m_0 increases, σ decreases and the relic density increases. Generically, supersymmetric particle masses cannot be too large if the universe is not to be overclosed by an excess dark matter ($\Omega > 1$).

In order to calculate the LSP relic density for all possible masses, one must consider a very large number of possible SUSY annihilation channels. In practice these contributions must be computed rapidly in order to explore wide regions of the multi-dimensional supersymmetric parameter space. An interesting solution, adopted by `micrOMEGAs`has been to rely on the `CompHEP` program [15] for computing the cross-sections. Loop corrections can be important in many cases, in particular those affecting widths of particles such as the Higgs. Use of one-loop results rather than a tree level treatment of the Higgs width can change the $\Omega_\chi h^2$ relic density value by a factor of two at large $\tan\beta$, due to the enhancement of the $b\bar{b}$ coupling. Thanks to efforts over more than a decade, the relic density can now be estimated from the electroweak scale MSSM parameters with an accuracy which in principle approaches 1%. However, supersymmetric threshold corrections will depend on the accuracy in determining the relevant SUSY particle masses. Also, the full QCD and the higher-order electroweak corrections need to be computed. If these are available by the time the LHC has collected a signifi cant data set, the intrinsic accuracy on the dark matter density extracted from the supersymmetric particle spectrum should be comparable to that expected from the next generation of satellite-borne CMB experiments.

As the SUSY particle masses increase, cosmologically viable solutions are possible only if the (co-)annihilation rates can be enhanced, for instance by accidental mass degeneracies. Furthermore, $\tilde{\chi}_1^0$ annihilation through resonances may take place at large velocities, thus requiring a relativistic treatment. A formalism for relativistic thermal averaging was developed in Ref. [16] and has been adopted by several programs.

If the LHC experiments are able to determine the masses and couplings of the SUSY particles, then the cold dark matter density can in principle be predicted using these software packages. A small change in the mass of the LSP may not have a signifi cant effect on the LHC phenomenology but can have a dramatic effect on the cold dark matter density. Conversely, the masses of heavier SUSY particles such as squarks and gluinos are very important at the LHC, as these are usually the dominant source of produced SUSY particles, while their masses are usually irrelevant to calculation of the relic density. A consistent attempt to reconcile LHC data with that from dark matter observations will require that the same model can be applied to both.

2.3. Cold Dark Matter in the Constrained MSSM

Within the constrained MSSM class of models the LSP is almost always the lightest neutralino. Cosmologically interesting LSP relic densities mostly occur only in certain regions of m_0-$m_{1/2}$ parameter space illustrated schematically in Figure 1. The region at low m_0 and $m_{1/2}$ is referred to as the "Bulk Region". Here there are no accidental degeneracies of the SUSY particles, no enhancements of σ and the LSP has a mass of less than 200 GeV. The region extending from the bulk region to large $m_{1/2}$, running along the edge where the slepton becomes the LSP has an enhanced annihilation rate as the lightest slepton and LSP are almost mass degenerate. This is known as the "co-annihilation tail". The region at large values of m_0 and $m_{1/2}$ is sometimes known as the "rapid annihilation funnel" or "Higgs pole region"

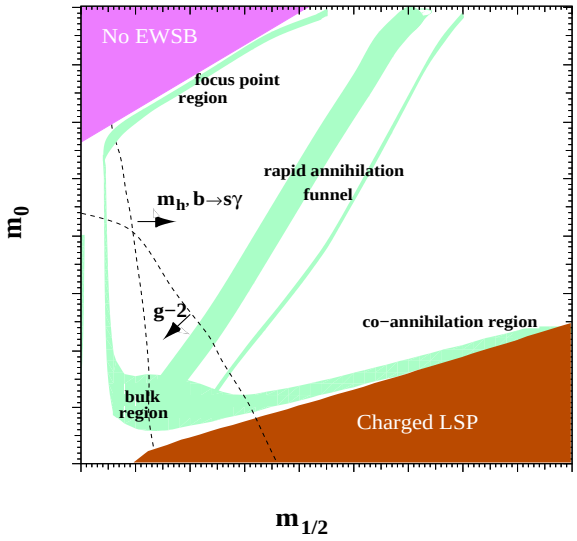

Figure 1. Schematic plot of the m_0-$m_{1/2}$ plane showing the regions where cosmologically interesting cold dark matter relic densities occur (light shaded regions). The dark region at low m_0 is excluded by the requirement that the LSP be neutral (here it is a charged slepton), while the dark region at large m_0 is excluded by the requirement that electroweak symmetry breaking occur. If SUSY is to explain the possible anomaly in the measurement of the muon anomalous magnetic moment [17], the region to the left of the $g-2$ line is preferred. A region at small $m_{1/2}$ is excluded by the direct limits on the Higgs boson mass [18]. The contribution from SUSY to the observed [19] decay $b \to s\gamma$ excludes the region at small masses unless the SUSY contribution is cancelled by other new effects.

and occurs when the mass of the LSP is such that annihilation via an intermediate (s-channel) heavy Higgs boson (A) enhances σ. Finally, at large m_0 there is the "focus point region" or "hyperbolic region" along the boundary beyond which electroweak symmetry breaking no longer occurs. We will now discuss in more detail the phenomenology of each of these regions. Note however that cosmologically interesting relic densities can also be generated in certain other scenarios, for instance when the LSP is nearly mass degenerate with the lighter stop squark at large A_0.

2.3.1. Bulk Region and Co-Annihilation Tail The region at low values of m_0 and $m_{1/2}$ corresponds to the largest area of the CMSSM parameter space yielding a cosmologically interesting cold dark matter relic density. In this region, the SUSY particles are relatively light and therefore the region is severely constrained by negative results of searches for supersymmetric particles at LEP-2 and the Tevatron. In the CMSSM, the Higgs mass is constrained to be less that 134 GeV [20]. Searches for the Higgs boson at LEP result in a lower limit on the Higgs mass of 114.4 GeV [18]. This and the lower limit on the chargino mass [7] reduce signifi cantly the allowed portion of this bulk region. Virtual effects from SUSY particles can affect the rates for certain rare processes. In particular, the observation of the loop-mediated $b \to s\gamma$ process provides a constraint which excludes small masses and is particularly important at negative μ and large values of $\tan\beta$. If SUSY is to explain the

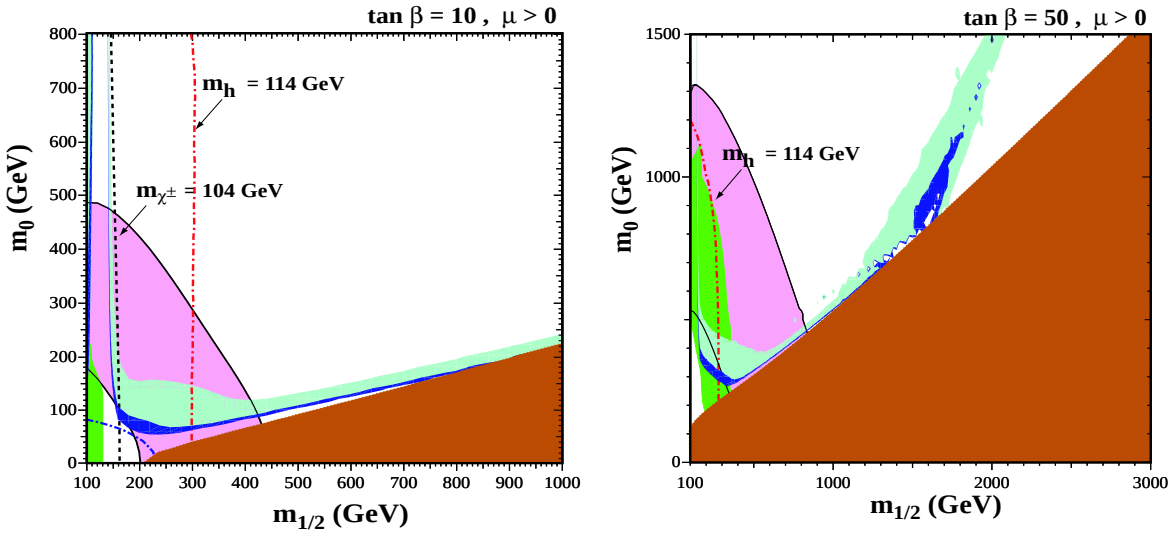

Figure 2. The m_0-$m_{1/2}$ plane for tanβ=10 (left) and 50 (right) showing the region allowed by WMAP data and the existing constraints from accelerator data. The "L"-shaped dark (blue) and light (cyan) regions correspond to $0.094 < \Omega_\chi h^2 < 0.129$ (WMAP) and $0.10 < \Omega_\chi h^2 < 0.30$ respectively. The regions on the left of the vertical lines are excluded by the LEP-2 limits on the chargino (dashed) and the Higgs (dashed-dotted) masses. The region below the lower (brown) triangle is forbidden since here the LSP is charged. From Ref. [21].

possible anomaly in the measurement of the muon anomalous magnetic moment [17], small masses are preferred.

As the masses of the SUSY particles increase, acceptable relic density is obtained by enhancing the annihilation rate. This happens in a narrow strip in the m_0-$m_{1/2}$ plane (the co-annihilation tail), where the $\tilde{\chi}_1^0\tilde{\tau} \to \tau\gamma$ co-annihilation process becomes enhanced due to near degeneracy between the masses of the $\tilde{\tau}$ and $\tilde{\chi}_1^0$ LSP. The precision of the WMAP measurement of $\Omega_\chi h^2$ has reduced the cosmologically allowed region to a very narrow one for each value of tanβ and sign of μ. The upper tip of this region, corresponding to the heaviest supersymmetric particle spectrum, is defined by its intercept with the slepton LSP ($m_{\tilde{\tau}} < m_\chi$) boundary. This is typically located at $m_{1/2} \sim O(1\text{ TeV})$. As we shall see below, this region can be entirely covered by LHC searches.

2.3.2. Focus Point Region In the focus point region at high m_0 the LSP changes its nature. Instead of being dominantly gaugino, as is the case elsewhere, it acquires a significant Higgsino content as μ is driven to small values [22]. At high values of tanβ the region where this occurs can lie at rather low values of $m_{1/2}$. As the Higgsino component can have a coupling to the SM gauge bosons, which is forbidden for the bino component by gauge invariance, σ is enhanced [23]. Furthermore the $\tilde{\chi}_1^0$ becomes nearly mass degenerate with the $\tilde{\chi}_1^\pm$ and $\tilde{\chi}_2^0$. Consequently a number of additional annihilation and co-annihilation processes contribute which together can reduce the $\tilde{\chi}_1^0$ relic density further to levels compatible with CMB data. Unlike the co-annihilation tail, the focus point region can extend to very large

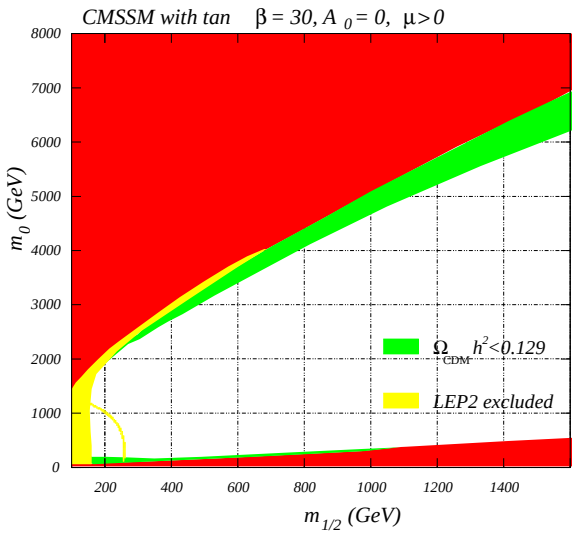

Figure 3. The focus point region in the CMSSM $m_0 - m_{1/2}$ plane for $A_0 = 0, \tan\beta = 10, \mu > 0$. The medium (green) region is consistent with WMAP relic density constraints ($0.094 < \Omega_\chi h^2 < 0.129$), while the light (yellow) region is excluded by LEP2 bounds. From Ref. [24]. See also Ref. [25].

values of m_0 leading to squarks, sleptons and gluinos that are too heavy to be observed at LHC.

The very existence of a cosmologically acceptable focus point region in CMSSM parameter space is sensitively dependent on the parameters describing the model, especially the top quark mass. In addition the large value of m_0 results in a "fine-tuning' problem; a delicate cancellation is required between different contributions to the Higgs potential to ensure that $M_Z << m_0$. This problem worsens as m_0 increases.

2.3.3. Higgs Pole Region When the value of $\tan\beta$ exceeds $\simeq 30$ another opportunity for enhanced $\tilde{\chi}_1^0$ annihilation is offered by the presence of heavy neutral Higgs particles, A^0 and H^0 with masses m_A such that $m_{\tilde{\chi}_1^0} \simeq m_A/2$. In this case the annihilation of lightest neutralinos is enhanced through resonant (s-channel) heavy Higgs exchange [26]. These processes can allow CMSSM models with m_0 and/or $m_{1/2}$ of order 1 TeV or greater to satisfy relic density constraints. The cosmologically acceptable region in these models takes the form of a "funnel" pointing toward large m_A defined by relic density contours passing around the annihilation pole. For values of $\tan\beta \gtrsim 60$ the coupling of the Higgs boson to bottom quarks becomes large and reliable computations are not possible.

2.4. Beyond the CMSSM

As the assumptions that lie behind the SUSY breaking in the CMSSM are relaxed, the range of SUSY particle masses for which there exists an acceptable dark matter candidate is considerably expanded. Within the CMSSM scheme, the assumption of the unification of the gluino and gaugino masses at a high scale ensures that the neutralino LSP is predominantly

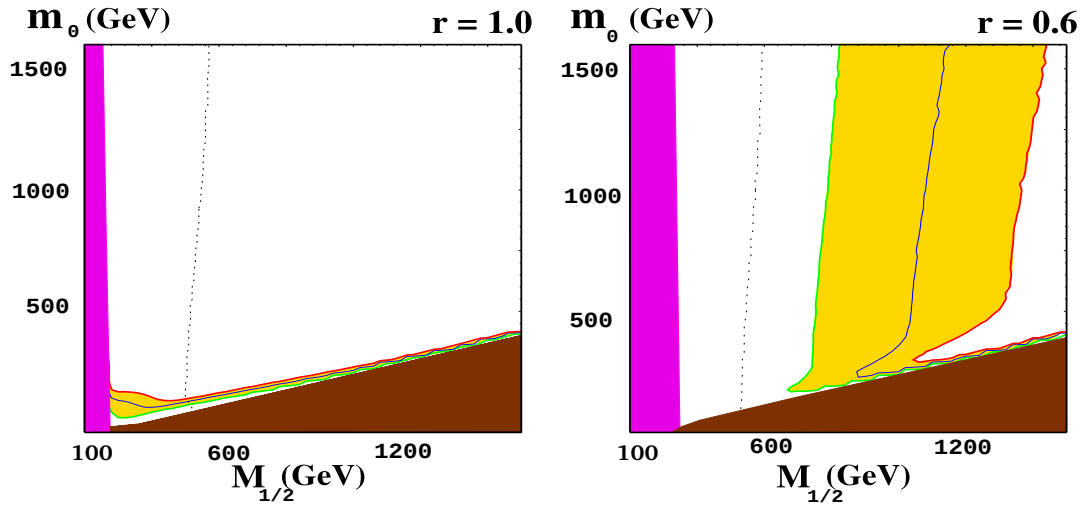

Figure 4. $\tilde{\chi}_1^0$ LSP relic density in the $m_0 - m_{1/2}$ plane for $\tan\beta = 5$ and differing gaugino mass assumptions. The cosmologically allowed relic density regions (light (yellow and green) shading) are displayed for $r = 1$ (left panel) and for $r = 0.6$ (right panel). Dark (brown) shaded regions in the lower right are excluded due to a charged LSP. Medium (pink) shaded regions on the left are excluded by LEP bounds on the chargino mass. The Higgs mass contour of $m_h = 113$ GeV is given by the dotted vertical line. Adapted from Ref. [27])

bino in the bulk region. If the LSP were dominantly wino on the other hand, it would have larger couplings and larger annihilation rates. Its mass could therefore be larger. This is illustrated in Figure 4 from Ref. [27] which shows the effect of changing $r = M_2/M_1$ from its unification value of $r = 1$. For $r = 0.6$ the LSP becomes wino-like and the bulk region expands as shown in the right hand plot.

The CMSSM also assumes that the soft scalar masses have a common value at the unification scale. This assumption can also be relaxed leading to modified relations between the squark, slepton and Higgs boson masses. This causes the LEP Higgs mass limit to no longer directly constrain the slepton and squark masses. The bulk region is not greatly affected by this modification, and the co-annihilation tail still exists, however the position and character of the focus point region can be radically altered since the squark and slepton masses no longer have to be large to obtain a small value of μ [28].

Another mechanism of SUSY breaking, "anomaly mediation" (AMSB) [34], results in a SUSY spectrum where the LSP is a wino. The simplest version of this class of models is ruled out as it predicts tachyonic sleptons, however variants can escape this constraint [35]. The characteristic feature of AMSB models is the near degeneracy of the LSP and the charged wino resulting in a large annihilation cross-section. Consequently if the LSP has a mass around 100 GeV far too few survive today to make a significant contribution to the dark matter. Nevertheless if the mass of the LSP is very large it is possible that a satisfactory dark matter density could be achieved.

In addition to gravity mediated models such as the CMSSM there also exists a class of gauge mediated SUSY breaking (GMSB) models [29, 30] in which the supersymmetry

breaking is mediated by gauge interactions. GMSB models assume that supersymmetry is broken with a scale $\sqrt{F}$ in a sector of the theory which contains heavy non-SM particles. This sector then couples to a set of particles with SM interactions, called messengers, which have a mass of order M. The mass splitting between the superpartners in the messenger multiplets is controlled by $\sqrt{F}$. One (two) loop graphs involving these messenger fields then give mass to the superpartners of the gauge bosons (quarks and leptons) of the SM. GMSB models are preferred by some because the superpartners of the Standard Model particles get their masses via gauge interactions, so there are no flavor changing neutral currents, which can be problematic in the CMSSM. The non-observation of supersymmetric particles and new particles associated with the messenger sector provides a bound on the SUSY breaking scale: $F \gtrsim \frac{4\pi}{\alpha_2} m_{\tilde{\chi}_2^+} M$ GeV^2 where $\alpha_2 \sim 1/28$ is the coupling strength of the $SU(2)$ electroweak interactions. Using $M, m_{\tilde{\chi}_2^+} > 100$ GeV implies $\sqrt{F} \gtrsim 2$ TeV however in most models F is at least ten times larger than this. Note that for gauge mediation to dominate F cannot be too large.

In GMSB models the characteristic spectra of superparticles are different from those found in CMSSM models. In particular the lightest supersymmetric particle is now the gravitino ($\tilde{G}$) whose mass is given by $m_{\tilde{G}} \sim \frac{\sqrt{F}}{100\text{TeV}}$ eV, implying that $m_{\tilde{G}} > 0.2$eV. The gravitino can have a mass of up to a GeV or so in specific models. It has feeble couplings and can be produced with significant rates only in the decays of particles which have no other decay channels. Its interactions are so weak that annihilation in the early universe typically only occurs via gravitational interactions and it falls very rapidly out of thermal equilibrium [31] leading to overclosure of the universe. This problem can be avoided if the temperature to which the universe is reheated after the end of inflation is sufficiently low to avoid over-production [32]. An alternative source of gravitino dark matter is non-thermal production in which the next to lightest SUSY particle (NLSP), which is usually a slepton or bino, decays to the gravitino. The lifetime of the NLSP can be sufficiently long for it to be effectively stable as the universe evolves, decaying only later to produce gravitino dark matter, long after it has fallen out of thermal equilibrium [33].

In certain SUSY models it is possible for the LSP to be a sneutrino. This is however not favored in most models as the sneutrinos are usually heavier than the right handed sleptons due to the their larger gauge couplings. Nevertheless a stable sneutrino is a good dark matter candidate [36] providing its mass is around 500 GeV [37]. Interaction rates of sneutrinos in direct detection experiments (see Section 5) are expected to be similar to those of heavy neutrinos of the same mass. Consequently current bounds from these experiments rule out sneutrino dark matter for sneutrino masses less than 1 TeV [38].

There are a small number of SUSY models in which the gluino is the LSP [39], however these are rare since ordinarily the larger coupling strength of QCD drives the gluino to larger masses than the other gauginos. Gluino LSPs produced thermally in the early universe are also unlikely to contribute significantly to the dark matter because they annihilate very efficiently via strong interactions leading to a number density typically of order 10^{-10} that of baryons. Gluinos cannot therefore account for a significant part of the dark matter unless they are produced non-thermally.

So far we have mostly assumed that the LSP was initially in thermal equilibrium. If this was not the case, then the prediction of its relic abundance is no longer valid. In particular it has been pointed out that the decay of "moduli fields" expected in some unification models can produce too many LSPs [40]. In gauge mediated scenarios, the excess production of gravitinos restricts the range of allowed masses [41]. In the case of anomaly mediation, it has been suggested that this mechanism can produce sufficient LSPs to obtain the correct relic density for LSP masses around 100 GeV [42].

3. LHC measurements of SUSY Dark Matter Properties

3.1. Inclusive Searches

The first issue is the reach of the LHC experiments for discovering supersymmetry. The reach is dependent on the details of the SUSY model, however the characteristic signals of missing transverse energy (from invisible LSPs), a large multiplicity of hadronic jets (from decays of squarks and gluinos) and/or isolated leptons (from decays of sleptons and gauginos) are sufficient to ensure detection over a large mass range. The left plot in Figure 5 shows the expected sensitivity of the CMS detector via the *Jets* + E_T^{miss} search channel to models in the CMSSM m_0-$m_{1/2}$ plane as a function of the integrated luminosity. About 30 fb^{-1} of data ensure that a signal can be observed over the whole extension of the co-annihilation tail. The right plot of Figure 5 shows the sensitivity with 100 fb^{-1}, in a variety of channels characterised by the number of observed isolated leptons. The most sensitive channel is that with jets and missing transverse energy and no isolated leptons labelled "0l". Signals with two isolated leptons of the same charge (marked "2l SS") can arise from the pair production of gluinos and their subsequent decay to charginos. Since the gluino is a Majorana fermion, it can decay into charginos of either charge. Their decays then give rise to this signal. Signals with two isolated leptons of opposite charge (marked "2l OS") arise from the same source but also from decays of the type $\tilde{\chi}_2^0 \to \ell\ell\tilde{\chi}_1^0$. Trilepton events (marked "3l") arise predominantly from events containing $\tilde{\chi}_2^0$ and a chargino.

3.2. Measurement of Cold Dark Matter Properties

The observation of signals characterized by large missing transverse energy, jets and/or isolated leptons at the LHC will give a strong indication that supersymmetry or some other New Physics resembling SUSY such as UED (Section 4) is present. It will also provide circumstantial evidence that *R* parity is conserved. The limited sensitivity of LHC experiments to the LSP lifetime ($\tau_\chi \gtrsim 1$ ms [44]) means that final confirmation that cold dark matter is supersymmetric in nature will require observation of signals in astroparticle experiments consistent with mass and cross-section predictions derived from LHC measurements. This is especially important given that the dark matter relic density measured by CMB experiments could consist of non-supersymmetric components in addition to that provided by the LSP. It will therefore be vital to measure sufficient SUSY parameters to verify consistency of

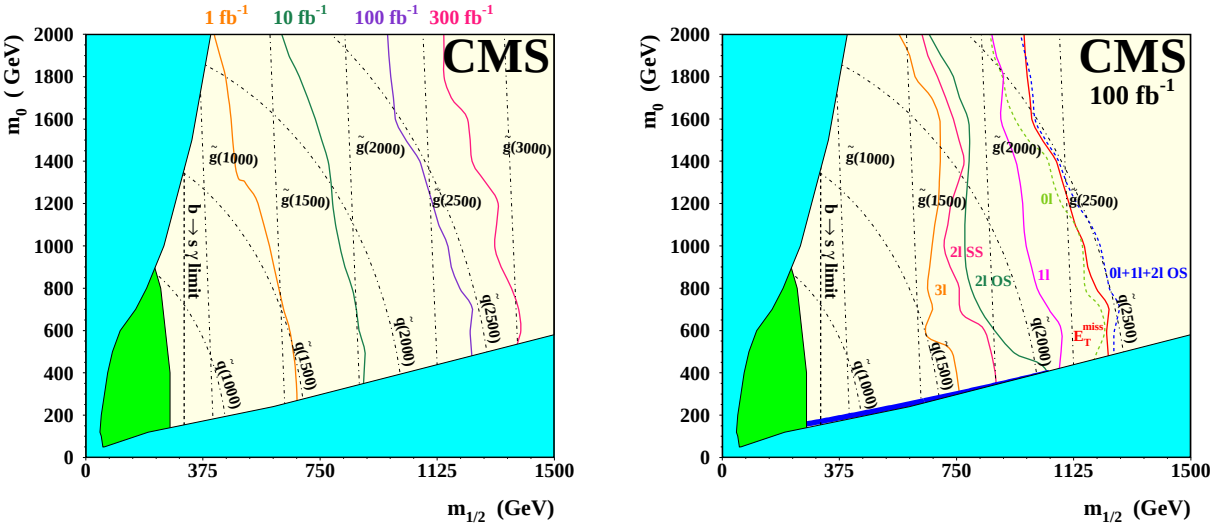

Figure 5. Sensitivity of LHC experiments to supersymmetry in the CMSSM m_0-$m_{1/2}$ plane. Left: reach of the *Jets* + E_T^{miss} search channel to obtain a 5 σ sensitivity for different integrated luminosities shown as solid lines. The dashed lines show fixed values of the squark and gluino masses. Right: reach of different search channels for 100 fb^{-1} of data indicated by the solid lines The cosmologically preferred region is indicated by the dark (blue) line extending over the excluded region where the LSP is charged (adapted from Ref. [43]).

the observed signals not only with CMB data but also with signals in these non-accelerator experiments.

Initially these measurements will be performed within the context of a specific SUSY breaking model, such as the CMSSM, by comparing significances in the various inclusive *Jets* + E_T^{miss} + *n leptons* channels discussed above. As more data accumulates, it will be possible to begin to reconstruct SUSY particle decays. This may enable model-independent measurement of the masses of some SUSY particles. However this will not necessarily be sufficient to provide a model-independent prediction of the dark matter relic density or other dark matter properties. This is because we do not know *a priori* which annihilation and co-annihilation processes dominated in the early universe, or equivalently in which region of which parameter space Nature's chosen model lies. With only limited knowledge of the SUSY mass spectrum it will therefore be necessary initially to assume a specific SUSY breaking model. This will enable the full SUSY mass spectrum to be obtained from a limited set of measurements, with additional input coming from the unification assumptions. Only once detailed model-independent measurements of more of the individual SUSY masses and couplings have been made can this model-dependency in the estimates of dark matter properties be reduced or eliminated.

As SUSY events will each contain two invisible LSP's, it will not possible to fully reconstruct the final states in these events. Measurements using exclusive channels will therefore focus on identifying key features of the SUSY particle decays. This typically

involves measuring the end-points and shapes of invariant mass distributions of leptons and jets arising in the decay of SUSY states [44, 45, 46]. Measurement of CMSSM model parameters can be accomplished through a global fit of the parameters to the positions of these edges, while model-independent mass measurements can be obtained by solving the various mass relations simultaneously.

The exclusive measurements which can be used to estimate dark matter properties in either a model-dependent or model-independent fashion depend strongly on the (co-)annihilation processes which drove the reduction of the dark matter density in the early universe. Within the context of the CMSSM the regions of parameter space where these different processes dominate correspond those discussed in Section 2.3. We shall therefore now discuss the measurements which can be made in each of these regions.

3.2.1. Bulk Region and Co-Annihilation Tail In the bulk and co-annihilation regions of CMSSM parameter space the mass of at least one of the sleptons or staus lies between that of the $\tilde{\chi}_2^0$ and the $\tilde{\chi}_1^0$ (LSP). The production of supersymmetric particles is dominated by squarks and gluinos as these have strong interaction couplings. If gluinos are heavier than squarks then they decay to squarks. In these regions there is a significant decay rate for $\tilde{q} \to q\tilde{\chi}_2^0 \to q\tilde{\ell}^{\pm}\ell^{\mp} \to q\ell^{\pm}\ell^{\mp}\tilde{\chi}_1^0$ and/or the equivalent stau channel. This decay chain gives rise to a jet, from the quark, a dilepton pair of the same flavor and opposite charge, and missing energy, from the $\tilde{\chi}_1^0$. After events are selected to contain a pair of isolated leptons, jets and missing energy, the left plot in Figure 6 shows the dilepton invariant mass distribution for a typical model. A clean structure is visible with a kinematic end point arising from this decay chain. Events beyond the end-point are due to other SUSY particle decays. The position of this end-point is determined by the masses of $\tilde{\ell}^{\pm}$, $\tilde{\chi}_2^0$ and $\tilde{\chi}_1^0$. If events are selected with a dilepton pair below this end point and this pair is then combined with all possible jets in the event, the mass distribution of the jet-dilepton combination with the lowest mass displays a kinematic structure whose end-point depends also on the quark mass (Figure 6 (right)). There is also a minimum value of the mass of the dilepton and jet and an upper value of the mass of a jet and single lepton.

These four quantities can be used to solve for the four masses: $\tilde{q}$, $\tilde{\ell}^{\pm}$, $\tilde{\chi}_2^0$ and $\tilde{\chi}_1^0$. It is important to note that a model is not required; simply the decay chain must be identified. When the masses are extracted precisions ranging from $\sim$ 3 % for the $\tilde{q}_L$ to $\lesssim$ 14 % for the $\tilde{\chi}_1^0$ for the LHCC Point 5 benchmark model are obtained [47]. Note however that the errors are strongly correlated as is illustrated in Figure 7: an independent measurement of one mass improves the precision on all of the others. Note also that when stau co-annihilation dominates, the above signatures can involve very soft taus which can be difficult to observe or measure with significant accuracy. Nevertheless if the mass difference between the $\tilde{\tau}_1$ and either of the lighter neutralinos is more than a few GeV then it should be possible to make at least a rough estimate of the relevant end-point positions.

Initial model-dependent (see Section 3.2) predictions for dark matter properties can be obtained from measurements such as these in two different ways. One approach is to fit the parameters of the assumed SUSY breaking model to the measured model-independent

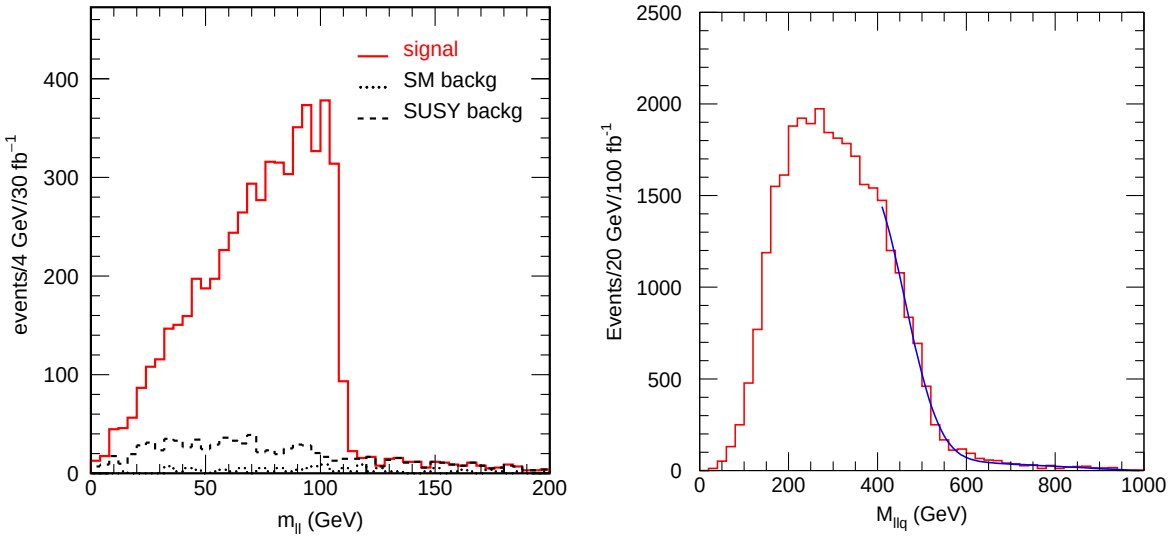

Figure 6. Invariant mass distributions obtained from the LHCC Point 5 benchmark model ($m_0 = 100$ GeV, $m_{1/2} = 300$ GeV, $A_0 = 300$ GeV, $\tan\beta = 2.1$, $\mu > 0$) for 100 fb^{-1} of data. Left: the invariant mass of a pair of opposite sign same flavor leptons arising from squark decay. Right: the invariant mass of a pair of opposite sign same flavor leptons and jet arising from squark decay. From Ref. [44].

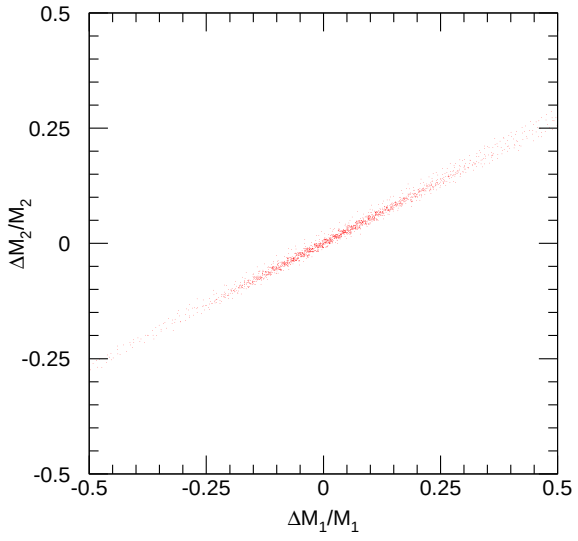

Figure 7. Plot showing errors on masses determined from the distributions in Figure 6. Note the strong correlation. From Ref. [44].

SUSY particle masses. The model parameters thus obtained can then be varied within their statistical and systematic errors to produce a probability density function for *e.g.* $\Omega_\chi h^2$ (left hand plot in Figure 8). This approach however does not take into account the correlations between the errors on the different measurements. An alternative approach which does take these correlations into account is to perform a global fit of the model parameters directly to all the end-point measurements prior to calculating the $\Omega_\chi h^2$ PDF (right hand plot in Figure 8). For the SPS1a bulk region benchmark model [48] a recent study [49] has shown that with 300 fb^{-1} of data statistical measurement precisions $\sim$ 2%, 0.6%, 9% and 16% can be obtained for the CMSSM parameters m_0, $m_{1/2}$, $\tan\beta$ and A_0 respectively. The sign of μ is also well-determined from the fit. It is estimated that $\Omega_\chi h^2$ can be pedicted with a statistical(systematic) precision $\sim$ 2.8% (3.0%). Further dark matter properties such as the spin-independent $\tilde{\chi}_1^0$-nucleon elastic scattering cross-section σ_{si} (see Section 5) are estimated with statistical precisions $\lesssim$ 1%, far smaller than the estimated factor $\gtrsim$ 2 systematic uncertainties in these quantities.

Full model-independent estimation of the dark matter density will require use of the model-independent mass values discussed above together with other measurements of quantities such as the masses of the lighter staus, heavy Higgs bosons and heavier neutralinos in order to show that slepton or stau (co-)annihilation dominates in the early universe (i.e. that the model does not lie near the heavy Higgs pole, or in the Focus Point region). More work on this subject is required.

3.2.2. Focus Point Region The phenomenology of the focus point region differs from that of the bulk and co-annihilation regions primarily due to the large masses of the sfermions. Depending on the parameters, the LHC may perform measurements providing some constraints on the dark matter density, or only observe an excess of events due to supersymmetry, or even, at the upper end of the parameter range, not observe supersymmetry at all. Sequential two-body, slepton-mediated, decays of $\tilde{\chi}_2^0$ to $\tilde{\chi}_1^0$, which form the basis of the measurements discussed previously, are kinematically suppressed. Some other signatures may still observed in these models, depending on the value of $\Delta m = m_{\tilde{\chi}_2^0} - m_{\tilde{\chi}_1^0}$.

In models with $\Delta m < m_Z$, such as the LHCC Point 4 model (m_0 = 800 GeV, $m_{1/2}$ = 200 GeV, $\tan\beta$ = 10, $\mu > 0$, A_0 = 0; not strictly speaking a focus point model but a good example of a model with $m_0 >> m_{1/2}$) studied in Ref. [51, 44], the $\tilde{\chi}_2^0$ decays almost exclusively to three-body final states involving a $\tilde{\chi}_1^0$ and two opposite-sign same-flavor leptons or quarks. The dilepton signature is easiest to identify and provides an invariant mass end-point sensitive to Δm which can be measured with subtraction techniques [44]. Combination of the dilepton pair with a hard jet may also give sensitivity to the $\tilde{q}_L$ mass while m_0 is sufficiently small for $\tilde{q}_L$ production to be significant. The mixed Higgsino-gaugino nature of the heavier neutralinos and charginos leads to significant couplings to the Z^0, and h^0 bosons, giving a characteristic Z^0 peak in the dilepton mass spectrum. The production cross-section and p_T distribution of these Z^0 bosons can be used to constrain heavier neutralino and chargino masses [44]. Further mass constraints were also obtained from a dijet invariant mass end-point sensitive to $m_{\tilde{g}} - m_{\tilde{\chi}_2^0}$, albeit with potentially large combinatorics. Sensitivity

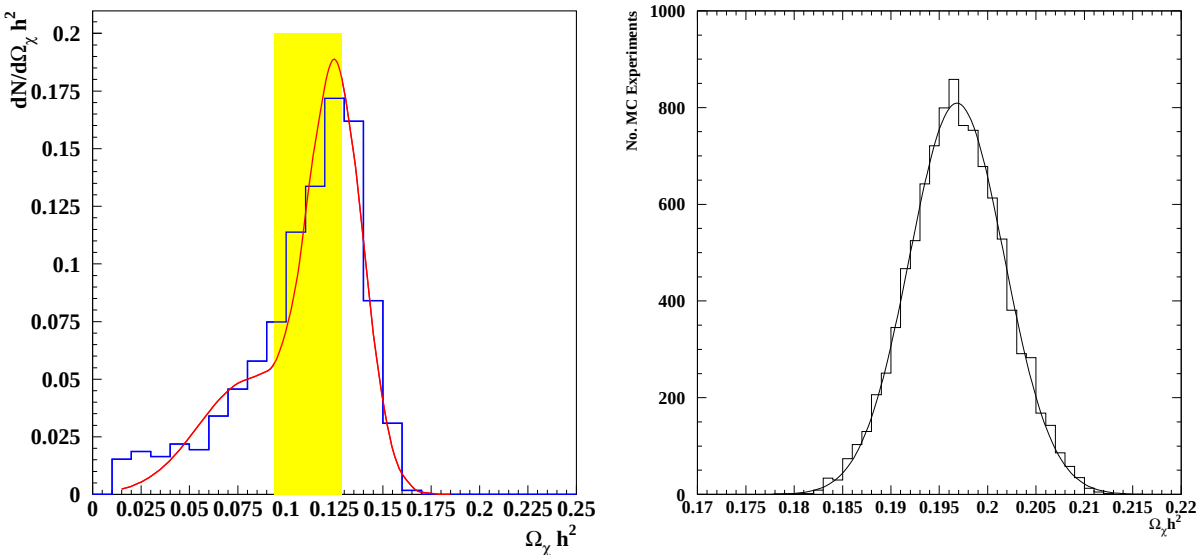

Figure 8. Probability density functions for the dark matter density as can be determined at the LHC. The left-hand distribution shows dark matter densities calculated from post-LEP benchmark model B' [50] by first fitting to invariant mass edges with model-independent SUSY particle masses, and then fitting CMSSM parameters to the measured mass distributions, before using those parameter values to calculate $\Omega_\chi h^2$. The range $0.094 < \Omega_\chi h^2 < 0.129$, favoured by WMAP, is shown for comparison. The right-hand distribution was obtained from the SPS1a benchmark model [48] by directly fitting CMSSM parameters to the invariant mass edges before using those parameter values to calculate $\Omega_\chi h^2$ (from Ref. [49]).

to squark and other sfermion masses is however difficult to obtain.

Model-dependent techniques, such as the analysis of the shape of the E_T^{sum} distribution of SUSY events, are then required. A combined fit of CMSSM parameters to the results of all the available measurements for LHCC Point 4, gave a precision $\sim$ 6% for m_0, $\sim$ 1% for $m_{1/2}$ and $\sim$ 15% for $\tan\beta$ (300 fb^{-1}). Unsurprisingly, the m_0 measurement precision was relatively poor compared with that for $m_{1/2}$ due to the difficulty of identifying and measuring the sfermion signals. The lack of sensitivity to A_0 and sign(μ) in this study indicates that only an order of magnitude estimate of $\Omega_\chi h^2$ could be obtained.

In the parameter region where $\Delta m > m_Z$ two-body decays of $\tilde{\chi}_2^0$ to $\tilde{\chi}_1^0 + Z^0$ and, for $\Delta m > m_h$, $\tilde{\chi}_1^0 + h$ become accessible. Phase-space suppression of the three-body $\tilde{\chi}_2^0$ modes and dominant $\tilde{\chi}_2^0$ production in complex $\tilde{g}$ three-body decays involving heavy flavors means that, even if an inclusive signal is observed, it is difficult to find mass distributions providing measurable end-points with little combinatorial background. Parameter measurements must therefore rely upon other techniques involving the Z^0 or h signatures. This is an area where further study is still required to assess the LHC potential.

The large masses of the strongly interacting particle partners cause an increasing fraction of the total SUSY production cross-section to be taken up by direct production of neutralinos and charginos. These events are characterised by little jet activity with instead multi-leptons,

or soft b-jets, arising for instance from Z^0 or h decay. Interest in specific searches for these signatures has been re-awakened by results of a recent study [52]. It indicates that the reach in the focus point region of gaugino searches at a 1 TeV e^+e^- linear collider, where gaugino pair production can be detected easily, can be greater than that of the LHC, when using the conventional jets + E_T^{miss} channels. At the LHC the production cross-sections for the electroweak gauginos in the focus point region are comparatively large, and the SM backgrounds, with appropriate cuts, can be made much smaller. The disadvantage of these channels is that hard cuts on jet activity are required to reject hadronic backgrounds leading to low efficiency and potentially large systematics due to poor understanding of mini-jet backgrounds from pile-up and the underlying event. These searches resemble those performed at the Tevatron. The characteristic signatures are dileptons or trileptons + E_T^{miss} arising from the production of electroweak gauge bosons in gaugino decay. In an early study of these channels [53] a plausible central jet p_T cut of 25 GeV was assumed, consistent with that used in more recent central jet veto studies for Higgs searches in the vector boson fusion channel [54]. Only limited sensitivity to the high m_0 region was found. However with a more refined analysis and a finer granularity scan of the narrow focus point region it may be possible to improve the reach of the method.

At very large values of m_0 and $m_{1/2}$, the $\tilde{\chi}_1^0$ becomes almost pure Higgsino and the $\tilde{\chi}_1^\pm$ can be almost mass degenerate with it (the so-called "inversion region" of the hyperbolic branch [25]). In this scenario, $m_{\tilde{\chi}_1^\pm} - m_{\tilde{\chi}_1^0}$ and $m_{\tilde{\chi}_2^0} - m_{\tilde{\chi}_1^0}$ are once again small and the two-body gauge and Higgs boson decay channels are closed. Three-body decays again dominate, however the chargino and neutralino mass differences can be such that only very low p_T leptons and jets are produced (although the NLSP does decay inside the detector [25]). Triggering upon such events is likely to be very difficult at the LHC, and measurement of sparticle masses still more so. The limited scope for SUSY particle mass measurement in this region means that estimation of the $\tilde{\chi}_1^0$ relic density is a difficult task. This problem is compounded by the fact that in this scenario the value of $\Omega_\chi h^2$ is strongly dependent on the top mass, which will only be known to a systematics-limited accuracy ~ 2 GeV at the LHC, after one year of low luminosity running [55].

Following any SUSY discovery at the LHC, the first indications that the focus point scenario is realised would likely come from a comparison of signal significance in different inclusive channels distinguished by the required number of leptons. In particular the signal significances in the jets + E_T^{miss} + $n \geq 1$ lepton channels are enhanced relative to that in the $n = 0$ leptons channel in the focus point region due to the abundant production of heavy flavors in gluino decay and leptons in chargino and neutralino decays via gauge bosons. Further evidence could then be provided by exclusive channels. At low Δm evidence for a di-lepton/di-tau end-point can be observed with a lepton/tau p_T asymmetry consistent with three-body decays [43], while at high Δm no evidence for such an end-point would be observable.

Relic density estimation within the CMSSM framework at low Δm would require use of the mass measurements and model parameter fitting techniques discussed above. At high Δm, $m_{1/2}$, $\tan\beta$ and sign(μ) could potentially be estimated from measurements involving direct chargino/neutralino production. But without an accurate estimate of m_0, the magnitude of

$\Omega_\chi h^2$ would be difficult to assess.

Estimation of the $\tilde{\chi}_1^0$ relic density in a more model-independent manner in the focus point scenario is even more difficult. Quantities which would need to be measured include the neutralino mass matrix parameters M_1, M_2, $\tan\beta$ and μ, and m_A. While it may be possible to measure some or all of the neutralino/chargino sector parameters from direct production studies (high Δm), the A may well be inaccessible to direct study (via e.g. $H/A \to \tau\tau$) due to its very high mass at high m_0. However, if $H/A \to \tau\tau$ were observed then this would enable a rather accurate measurement of $\tan\beta$ to be performed [56].

3.2.3. Higgs Pole Region The potentially very large masses of the strongly interacting super-partners in these "rapid-annihilation" models means that, if realized in nature, their discovery at the LHC is by no means guaranteed (see, for example, the benchmark model "M" in Ref. [50]). Nevertheless, if their spectrum is within reach of the LHC, it may be possible to measure many of the model parameters through the use of invariant mass end-point techniques. The rapid-annihilation funnel region in general occurs in the high $\tan\beta$ $m_0 - m_{1/2}$ plane relatively close (in all but the highest $\tan\beta$ scenarios) to the stau co-annihilation tail discussed in Section 3.2.1. Consequently for many rapid-annihilation models the $\tilde{\tau}_1$ is light and $m_{\tilde{\tau}_1} < m_{\tilde{\chi}_2^0}$. Ditau signatures may therefore be used to identify SUSY events containing $\tilde{\chi}_2^0$ decays, and fits to invariant mass thresholds and end-points involving one or more of these taus used to constrain either CMSSM parameters or model-independent SUSY particle masses. This analysis should be somewhat easier than in the stau co-annihilation case (for the same total SUSY cross-section) since here the $\tilde{\tau}_1 - \tilde{\chi}_1^0$ mass difference is greater and hence the taus from the $\tilde{\tau}_1$ decays have greater p_T.

In addition to ditau production further signatures can be used to identify and measure SUSY events in rapid-annihilation models. These models in general possess relatively large values of m_0 compared with those of models in the stau co-annihilation tail, and this enhances the Higgsino content of the lighter neutralinos and hence the branching ratio of $\tilde{\chi}_2^0 \to Z^0/h + \tilde{\chi}_1^0$. This allows further constraints to be placed on masses through identification of Z^0 and h^0 production in high E_T^{miss} events [57] and then measurement of invariant mass end-points in $Z^0 q$ and hq invariant mass distributions. Additional constraints can be obtained by searching for $\tilde{q}_R \to \tilde{\chi}_1^0 q$ decays producing dijets + E_T^{miss}, which give sensitivity to the $\tilde{q}_R$ mass [24, 57]. Given an estimate of the mass of the $\tilde{\chi}_1^0$ from e.g. the ditau analysis the measurement can be performed either by analyzing the shape of the p_T distribution of each of the jets [57, 44] or by fitting to the end-point of the distribution of the dijet m_{T2} variable [47, 58].

A case study of CMSSM parameter fitting in a model with this phenomenology is the analysis of LHCC Point 6 (m_0 = 200 GeV, $m_{1/2}$ = 200 GeV, $A_0 = 0$, $\tan\beta = 45$, $\mu < 0$) described in Refs. [59, 44]. By using a combination of measurements of m_h and $m_{\tilde{q}_R}$, constraints on $m_{\tilde{g}}$ and $m_{\tilde{g}} - m_{\tilde{b}_1}$ obtained from $\tilde{g}$ decays to $\tilde{b}_1 b$, and fits to the ditau end-point, measurement precisions $\sim$ 12%, 5% and 4% were obtained for m_0, $m_{1/2}$ and $\tan\beta$ respectively. However, the analysis was relatively insensitive to A_0 and the sign of μ, which would limit the predictivity of these data in estimating the relic density.

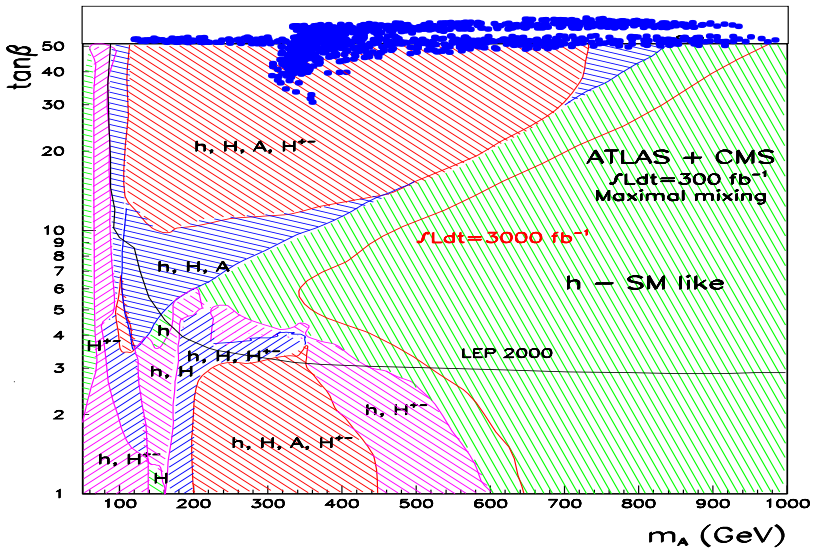

Figure 9. Estimated number of Higgs bosons observable at the LHC in the M_A, $\tan\beta$ plane. The cosmologically interesting solutions belonging to the A funnel regions obtained with a parameter scan are shown by the dots. In the relevant region of parameters, the LHC will be essentially observing all the Higgs bosons.

In models with very large $\tan\beta$ it is possible for the rapid-annihilation funnel to be sufficiently wide for the cosmologically-allowed region on the high m_0 side of the base of the funnel to lie in the region where $m_{\tilde{\tau}_1} > m_{\tilde{\chi}_2^0}$. The phenomenology of such models resembles more closely that of the focus point models discussed in Section 3.2.2, with characteristic $Z^0/h + E_T^{miss}$ ($\Delta m > m_Z$ or m_h) or ditau + E_T^{miss} ($\Delta m < m_Z$) signatures arising from $\tilde{\chi}_2^0$ decay.

Given a set of measurements of CMSSM parameters from the above analyses it should be relatively straightforward to calculate the $\tilde{\chi}_1^0$ relic density, although the resulting error could well be significant due to its strong dependence on both SUSY and SM (m_{top}) input parameters [21]. In order to obtain a more model-independent estimate of the relic density it will be necessary first to confirm that $\tilde{\chi}_1^0$ annihilation in the early universe was dominated by resonant s-channel A production. Assuming that the $\tilde{\chi}_1^0$ mass has been determined through the ditau + E_T^{miss} analysis m_A must now be measured independently through a search for e.g. $H/A \to \tau\tau$ or (better) $H/A \to \mu\mu$ to check that $m_A \simeq 2m_{\tilde{\chi}_1^0}$. It is interesting to observe that in the CMSSM parameter region where a cosmologically interesting CDM density is achieved due to the rapid $\chi\chi$ annihilation process through the A^0 pole, the LHC should observe the A^0 and H^0 bosons for masses at least as high as 800 GeV [60], corresponding to $m_{1/2} \sim 950$ GeV with 300 fb^{-1} integrated luminosity (see Figure 9). An LHC upgrade, increasing the luminosity by an order of magnitude, would ensure that the whole region is covered. The A mass measurement accuracy depends crucially on the availability of the $A^0 \to \mu\mu$ channel in which case a $O(0.1\%)$ precision can be reached with 300 fb^{-1} ($\delta m/m \sim 0.1\%$ for m_A = 300 GeV at $\tan\beta$ =30) [56]. In these cases $\tan\beta$ could also be measured to a precision $\sim 5\%$ [56]. At the largest values of m_A, where only the $A^0 \to \tau\tau$ is available, the accuracy on m_A will be typically

of the order of a few %, limited by energy calibration systematics.

3.2.4. Other Scenarios Measurements of SUSY parameters and hence dark matter properties in other non-CMSSM scenarios have been studied in far less detail. If the LSP is a wino then evidence could be provided by studying the branching ratios of the $\tilde{\chi}_2^0$ and $\tilde{\chi}_1^0$, as well as measuring the full neutralino mass matrix. Given a plausible model such as that studied in Ref. [27] it may then be possible to measure sufficient parameters to estimate $\Omega_\chi h^2$. Similarly if the LSP is a sneutrino then this will significantly alter the cascade decay chains used in the CMSSM analysis but not prevent observation of the kinematic end-points used to constrain masses or model parameters. If a GMSB model is realised in nature then the prospects for direct detection (Section 5) are slim, but studies at the LHC will be fruitful with a wide variety of signatures and mass constraints accessible [44]. This should enable the GMSB model parameters to be estimated and, if the lifetime of the NLSP can be measured, it should be possible to estimate the SUSY breaking scale and hence the mass of the gravitino LSP.

4. Cold Dark Matter and Extra Dimensions

Extra dimensions offer an alternative solution to the hierarchy problem. Instead of introducing a cancellation of the divergences as in supersymmetry, extra dimensions bring the effective unification scale from the Planck to the TeV scale. Of the several models which have been proposed, Universal Extra Dimensions [61] are of particular interest here since they offer a cold dark matter candidate. The simplest realisation of UED has all the SM particles propagating in a single extra dimension of size R, which is compactified on a S_1/Z_2 orbifold. This single parameter determines the phenomenology of the model. Each Standard Model particle has an infinite tower of Kaluza Klein (KK) excitations, with each level one excitation possessing a mass equal to $1/R$ at tree level. This mass degeneracy is broken only by radiative corrections. A further specific feature of UED is the conservation of the Kaluza-Klein number at tree level. Radiative effects [62, 63, 64] break KK number conservation down to a discrete conserved quantity known as KK parity, given by $(-1)^n$ where n is the KK level. The level one KK states in UED models with conserved KK parity therefore strongly resemble the particles appearing in SUSY models with conserved R-parity and indeed it can be difficult to distinguish such models experimentally. The lightest KK partner (LKP) at level one is often neutral and has negative KK parity causing it to be stable on cosmological time scales. The LKP is therefore a plausible dark matter candidate again resembling LSP candidates.

In minimal UED models, the LKP is the KK partner of the electroweak hypercharge gauge boson B^0, denoted by $B^{(1)}$ [64]. The relic density of LKP dark matter lies in the range favoured by WMAP data if $1/R \simeq O(1\ TeV)$ [65]. The $\nu^{(1)}$ state, another possible candidate, is already excluded by present limits from direct detection experiments [66]. In the early universe $B^{(1)}B^{(1)}$ annihilation proceeds through the s-channel and is more efficient than in the SUSY neutralino case. The cosmologically interesting mass scale for the LKP is therefore significantly larger than that for supersymmetric candidates (see Figure 10), although it still

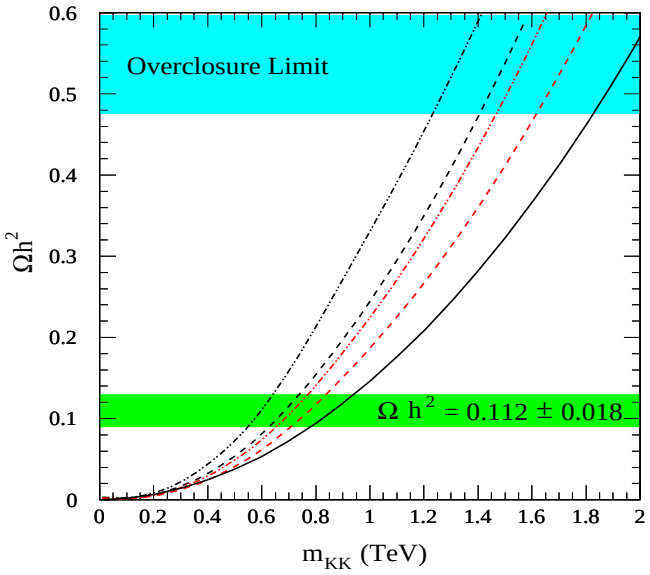

Figure 10. Relic dark matter density as a function of the UED mass scale $m_{KK} = 1/R$ corresponding to the mass of the level one KK states. The WMAP result is shown by the horizontal band. The solid line includes only the $B^{(1)}$ contribution. The dashed lines also include the effect of co-annihilations with one and three generations of lepton excitations for mass splittings of 1 % and 5 % (adapted from Ref. [65]).

lies well within the anticipated LHC reach of $\sim$ 1.5 TeV [67]. Co-annihilation with the $e_R^{(1)}$ state is possible if its mass is almost degenerate with that of the LKP however the UED co-annihilation cross-section is not sufficiently large to reduce significantly the $B^{(1)}$ density. The net result is that the dark matter density increases in the case of nearly degenerate states, since the $B^{(1)}$ and the $e_R^{(1)}$ decouple at about the same freeze-out temperature.

Kaluza-Klein dark matter also offers interesting prospects for direct or indirect detection at space- and ground-based experiments [66, 68]. Direct detection (see Section 5 for the SUSY case) proceeds through KK quark and Higgs exchange between relic LKPs and atomic nuclei and can give sensitivity to LKP masses in excess of 1 TeV for tonne scale experiments and favourably small values of the level one quark and $B^{(1)}$ mass difference.

There are three main indirect signatures which can be sought. The first consists of a peak of mono-energetic positrons which could be produced in $B^{(1)}B^{(1)} \to e^+e^-$ annihilation. The AMS experiment on the ISS should be able to distinguish positrons from photons up to about 1 TeV and consequently could provide a means to detect LKP dark matter for masses up to $\simeq$1000 GeV. A second signature is represented by an excess of photons, with a continuum spectrum, which could probe mass scales up to about 600 GeV. Finally high energy neutrinos could be detectable at foreseen experiments, with a sensitivity up to about 400 GeV.

Non-supersymmetric grand unified theories with warped extra dimensions also introduce a stable Kaluza-Klein state, which could be a candidate for cold dark matter. Such a state arises from imposing baryon number symmetry which is spontaneously broken at the Planck scale [69]. It has the quantum numbers of a right-handed neutrino and cannot decay into SM

particles. Depending on the other parameters of the model, there is a vast range of masses for this particle to produce the required dark matter density, from a few tens of GeV up to about 1 TeV or higher. At the LHC, a possible signature of such a scenario is provided by the production of the next-to-lightest KK particles which would have a sufficiently long lifetime to travel through the detector volume and be recorded as heavy stable particles.

The main feature of UED models, as well as SUSY models, which leads to the existence of a plausible dark matter candidate, is the existence of a conserved quantum number distinguishing the new states from those appearing in the SM. Conservation of these quantum numbers in general provides these models with additional attractive features [70]. This idea has been generalised to solve the so-called "little" hierarchy problem suffered by many models predicting new physics at the TeV scale [70]. In doing so a candidate dark matter particle is invariably produced. One test case considered by the authors of Ref. [70] was that of a little Higgs model, in which a Z_2 symmetry referred to as "T-parity" is imposed. The result is a dark matter candidate which is either the new B' gauge boson or a new $SU(2)_W$ singlet or triplet scalar particle. The annihilation of the former to SM particles is not chirally suppressed, unlike in *e.g.* SUSY models, and so indirect detection signatures are expected to be enhanced. Singlet scalar candidates have very small couplings to other states and must therefore be of very low mass ($\lesssim$ 100 GeV) to give an acceptable relic density [70]. States with a significant triplet component can interact with light gauge bosons, providing a mechanism for their annihilation in the early universe, and consequently their cosmologically allowed mass range is expected to be higher ($\gtrsim$ 500 GeV) [71].

5. Direct Detection of DM particles

5.1. Motivation

Although LHC experiments can provide supporting evidence for the existence of cold dark matter particles, their limited sensitivity to the lifetime of neutral particles (e.g. $\tau \lesssim 1$ ms for $\tilde{\chi}_1^0 \to \tilde{G}\gamma$ in GMSB SUSY models in ATLAS [44]) prevents them from providing conclusive proof. Similarly it is very difficult for astroparticle experiments to prove that any observed signal is due to a particular candidate, such as the LSP, rather than some other exotic form of new physics (*e.g.* UED). This means that in order to obtain a discovery of a specific new dark matter candidate *consistent* signals will need to be observed at *both* colliders such as the LHC *and* in astroparticle experiments.

There are two classes of astroparticle searches for cold dark matter; indirect searches seeking evidence of dark matter annihilation products such as neutrinos generated in the earth, sun or galactic center, or gamma rays or anti-matter generated in the galactic halo (see e.g. Ref. [23] and references contained therein), and direct searches sensitive to the elastic scattering of cold dark matter particles from atomic nuclei in earth-bound detectors [72]. In this review we concentrate on the latter, however it should be noted that the former can also provide very strong constraints and indeed may already have provided first evidence for particle dark matter in the form of an excess of positrons from the galactic halo [73].

5.2. Basics of Direct Detection

In direct searches, evidence for the existence of cold dark matter particles is provided by an observation of an anomalous source of recoiling nuclei inside a detector. The precise form of the recoil energy spectrum of the nuclei depends on factors arising from astrophysics (the local density and velocity distribution of incident dark matter particles), nuclear physics (form-factors and coupling enhancement factors for scattering at finite momentum transfer q) and particle physics (the particle mass and interaction cross-section). In general, the spectrum is expected to fall quickly with increasing energy due to the small average kinetic energy of the population of dark matter particles trapped within our galaxy (the galactic "halo"). This leads to a need for detectors with extremely low ($\sim$ keV) nuclear recoil energy thresholds. In addition, the nuclear scattering cross-section is strongly enhanced by a factor $\propto A_m^2$ (nuclear target mass squared) for spin-independent interactions (see below), favoring target materials incorporating high mass (large A_m) nuclei.

The main background to signal events due to nuclear recoils in these detectors arises from electron recoils generated by Compton scattering of gamma radiation from naturally occurring radio-nuclides in, and around, the target. It is therefore essential that detectors be shielded from external sources of gamma radiation, and that they be constructed from materials of the highest possible radio-purity. It is also most advantageous if detectors are designed to discriminate between nuclear recoil signal and electron recoil background events.

In addition to the electron recoil background there is also a potential source of irreducible background events from elastic scattering of neutrons from nuclear spallation by cosmic ray muons and decay of radio-nuclides from natural U and Th chains in the detector and its environment. The flux of spallation neutrons can be reduced to very low levels by installing detectors deep underground where the muon flux is minimal. Neutrons from radioactive decay are generally of lower energy and can be absorbed using hydrogenous shielding materials or tagged using active neutron vetoes.

5.3. Direct Searches and SUSY

Direct searches for cold dark matter rely upon the existence of weak-scale couplings between dark matter particles and quarks and gluons in the nucleus. The nature of these couplings depends strongly on the identity of the dark matter particle with scalar, axial-vector and vector couplings being important for different candidates [74]. Axial-vector currents couple to the distribution of spin in the nucleus and hence contribute to the *spin-dependent* elastic scattering cross-section. Scalar currents by contrast couple effectively to the mass distribution of the nucleus and contribute to the *spin-independent* elastic scattering cross-section. For non-Majorana dark matter particles vector couplings tracing the charge distribution of valence quarks in the nucleus can further contribute to the spin-independent cross-section [74]. It is important to note that the spin-independent cross-section is a measured quantity and is, in this case, not equivalent to the scalar cross-section, which must be calculated using model assumptions.

In gravity-mediated MSSM cold dark matter models the LSP can be the lightest

neutralino, a sneutrino, or possibly a light gluino (see Section 2.4). As noted above, the last possibility is heavily constrained and will not be discussed further. The sneutrino has a large coupling to ordinary matter and hence is almost excluded [37] by direct searches due to a large predicted vector coupling contribution to the spin-independent scattering cross-section. This leaves the Majorana $\tilde{\chi}_1^0$ as the most favored MSSM cold dark matter candidate.

In CMSSM models when the LSP is neutral it is always the $\tilde{\chi}_1^0$. At tree-level the scalar $\tilde{\chi}_1^0$-nucleus interaction receives contributions from $\tilde{q}-\tilde{\chi}_1^0$ couplings involving t-channel Higgs exchange or s-channel $\tilde{q}$ exchange. At 1-loop further signifi cant contributions can arise from diagrams coupling the $\tilde{\chi}_1^0$ to a gluon [75]. Axial-vector interactions arise from t-channel Z^0 exchange and s-channel $\tilde{q}$ exchange. The magnitudes of the scalar and axial-vector cross-sections depend on a number of SUSY parameters including the $\tilde{\chi}_1^0$ mass and composition (*i.e.* M_1, $\tan\beta$ and μ), the squark masses and the heavy Higgs mass m_A. In order to obtain a model-independent estimate at the LHC of the expected event rates in direct search experiments it will therefore be necessary to perform a wide range of SUSY particle mass measurements.

Within the CMMSM, typical values for the scalar $\tilde{\chi}_1^0$-nucleon interaction cross-section range from $\sim 10^{-6}$ pb to $\sim 10^{-8}$ pb in the focus point region, where $\tilde{\chi}_1^0\tilde{\chi}_1^0 A$ couplings are enhanced by the Higgsino content of the $\tilde{\chi}_1^0$ and Aqq couplings by the large value of $\tan\beta$ [76], to $\lesssim 10^{-10}$ pb in the co-annihilation tail [28]. When $\mu < 0$ it is possible for the u and d quark contributions to the scattering to interfere destructively reducing the cross-section still further [28, 77]. Large values of the scalar cross-section are also obtained in regions with small m_0 and $m_{1/2}$ where the squark mass is small leading to effi cient s-channel scattering. Similar arguments apply to the axial-vector $\tilde{\chi}_1^0$-nucleon cross-section, with values ranging from 10^{-4} pb in the focus point region, where the Higgsino content of the $\tilde{\chi}_1^0$ enhances the $Z^0\tilde{\chi}_1^0\tilde{\chi}_1^0$ coupling, down to 10^{-8} pb in the stau co-annihilation tail, where $m_{\tilde{q}}$ is large [77].

5.4. Prospects for Direct Searches

The current generation of direct search experiments have attained a sensitivity to the normalized spin-independent $\tilde{\chi}_1^0$-nucleon cross section $\sigma_{si} \sim 4\times 10^{-7}$ pb [78] (Figure 11). The DAMA experiment operating at the Gran Sasso underground laboratory [79] has claimed evidence for an annual modulation signature consistent with a cold dark matter interpretation ($m_{\tilde{\chi}_1^0} \sim 52$ GeV, $\sigma_{si} \sim 7.2\times 10^{-6}$ pb [83]), however the region of parameter space allowed by this data has now been largely excluded by other experiments [78, 80, 81, 82]. The region allowed by the DAMA data can be extended by varying the parameters of the velocity distribution of cold dark matter particles trapped within our galaxy [83], or by assuming contributions to the signal from both spin-dependent and spin-independent couplings [84]. Nevertheless it is not clear that these new regions of parameter space are not also excluded by other experiments when similar assumptions are made. Current limits on the spin-dependent $\tilde{\chi}_1^0$-nucleon cross-section σ_{sd} assuming a pure Higgsino LSP candidate (see below) are ~ 1 pb [87].

Within the next two years a new generation of high mass experiments capable of enhanced electron-recoil background discrimination will come on-line. These are sensitive

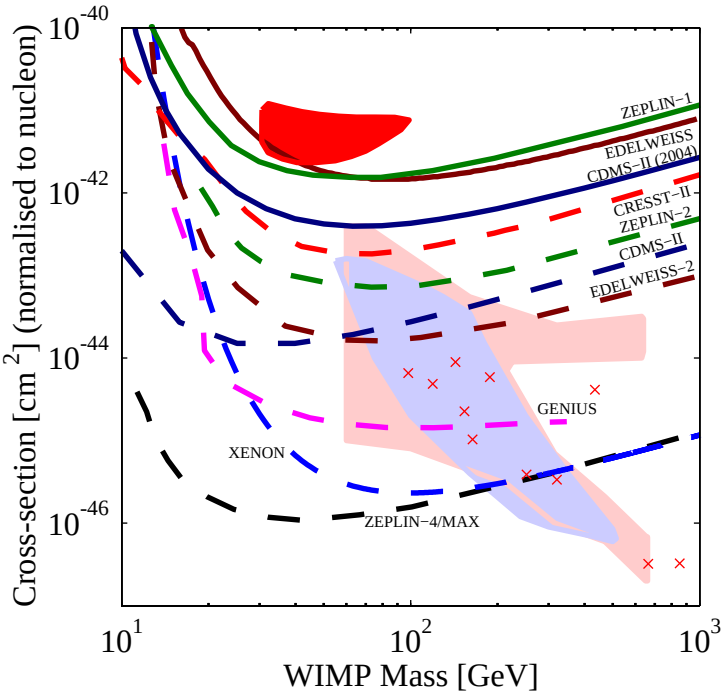

Figure 11. Sensitivities of some running and planned direct detection dark matter experiments to the spin-independent elastic scattering cross-section. Full curves correspond to limits from existing experiments (ZEPLIN-1 [82], EDELWEISS [81], CDMS-II (2004) [78]), dashed curves to predicted sensitivities of future experiments (next generation: CRESST-II [91], ZEPLIN-2 [88], CDMS-II [89] and EDELWEISS-2 [90]; tonne-scale: GENIUS [96], XENON [95] and ZEPLIN-4/MAX [93, 94]). The full dark (red) region corresponds to the 3 σ allowed region from the DAMA experiment [83]. The full light regions correspond to predictions by Chattopadhyay et al. [85] and Baer et al. [28] in the light of WMAP data. The crosses correspond to neutralino masses and cross-sections predicted for post-LEP benchmark CMSSM models [50]. Adapted from Ref. [86].

to spin-independent interaction cross-sections $\sim 10^{-8}$ pb after a few years of running [88, 89, 90, 91]. In the longer term, specific proposals are being made to build still larger tonne-scale experiments [92, 93, 94, 95, 96] capable of probing $\sigma_{si} \sim 10^{-10}$ pb at the lower limit of the CMSSM favored cross-section region (at least for $\mu > 0$). These experiments are likely to be particularly challenging because of the difficulty of ensuring that neutron-induced background events do not systematically limit detector sensitivity. It is likely that the neutron flux from external sources can be reduced to acceptable levels with active and passive shielding [97]. Reduction of the neutron flux from U/Th contamination of detector components will require careful design and material assay. This background will probably define the ultimate sensitivity of direct search experiments since even the purest detector construction materials will always contain some U/Th chain nuclides [97]. Improvements in the sensitivity to spin-dependent interactions can be expected to be similar to those for spin-independent interactions, however the lack of a cross-section enhancement due to nuclear

coherence [74] means that tonne-scale detectors will only be sensitive to $\sigma_{sd} \sim 10^{-5}$ pb, which is only just inside the CMSSM predicted range.

By 2011, when the LHC should have acquired 100 fb^{-1} of data, tonne-scale direct search experiments should have been running for a few years. By this stage therefore cold dark matter models predicting $\sigma_{si} \gtrsim 10^{-9}$ - 10^{-10} pb should have either been excluded or produced a signal in these experiments. This opens up the exciting prospect of complementary studies of particle dark matter using direct search data and exclusive measurements at the LHC.

6. Complementarity of Measurements

Direct search experiments are complementary to the LHC in several important ways. In terms of discovery of SUSY it is clear that direct searches are particularly sensitive to focus point models in which the $\tilde{\chi}_1^0$ acquires a significant Higgsino component. These are the same models however which the LHC will find hardest to discover due to the high masses and hence reduced production cross-sections of both squarks and gluinos. As a result the LHC and direct search discovery contours are roughly orthogonal in this region of parameter space and the latter could conceivably find evidence for BSM physics at mass scales in excess of 3 TeV with σ_{si} as high as 10^{-8} pb [28]. By contrast, in the co-annihilation tail the sensitivity of direct search experiments drops off rapidly with rising $m_{1/2}$ as $m_{\tilde{q}}$ increases, and here the LHC stands a much better chance of making a discovery.

In the event of discovery of signals at both the LHC and direct detection experiments further valuable cross-fertilization is possible. If the LHC experiments can measure the SUSY model parameters (*e.g.* m_0, $m_{1/2}$ etc. in the CMSSM) using the techniques described above then a model-dependent estimate of the spin-independent and spin-dependent elastic scattering cross-sections can also be obtained. It may also be possible to measure sufficient weak-scale SUSY parameters, including the neutralino mass matrix parameters together with m_A and $m_{\tilde{q}}$, to obtain a "model-independent" estimate of the cross-sections for comparison with direct search measurements. Note that the precision of these measurements will itself be ultimately limited by astrophysical model-dependence due to the unknown distribution of dark matter within the galactic halo. It is important to remember however that the direct search parameter space is defined both by the interaction cross-section and the dark matter particle mass. The kinematics of the elastic scattering process mean that for $\tilde{\chi}_1^0$ masses $\lesssim A_m$ (the mass of the target nucleus) the shape of the energy spectrum of signal nuclear recoils for scalar interactions is strongly correlated with the mass of the $\tilde{\chi}_1^0$ (for larger $\tilde{\chi}_1^0$ masses the energy spectrum tends to a limiting distribution insensitive to the mass value). This correlation is furthermore rather model-independent. Consequently for $\tilde{\chi}_1^0$ masses $\lesssim 180$ GeV ($\sim$ the mass of a tungsten nucleus, the heaviest nucleus used in current or proposed experiments [91]) it should be possible to measure the $\tilde{\chi}_1^0$ mass rather accurately without recourse to any particular model framework. This will then allow direct comparison with LHC results.

It is interesting to note that a good case study of a direct search mass measurement already exists in the form of the analysis performed by DAMA of their claimed annual modulation signal [79, 83, 84]. The soft energy spectrum observed in this experiment is

claimed to be consistent with a small $\tilde{\chi}_1^0$ mass considerably less than that of the ^{127}I target nuclei. Under this assumption therefore an accurate measurement of the $\tilde{\chi}_1^0$ mass can be performed giving a precision ~ 20 % (52^{+10}_{-8} GeV [83]).

LHC-direct search complementarity is likely to be even more pronounced if a spin-dependent dark matter signal is observed. In this case, there is a strong dependence of the relative magnitude of the axial-vector couplings of the $\tilde{\chi}_1^0$ composition to protons and neutrons [98] that can lead to significant model-dependence in the overall $\tilde{\chi}_1^0$-nucleus (or normalized $\tilde{\chi}_1^0$-nucleon) cross-section. Only in the pure Higgsino case is this model-dependence lifted. Direct search experiments can absorb this model-dependency into a redefinition of measured cross-sections in terms of cross-sections for scattering from protons and neutrons separately [98]. Only with the aid of LHC measurements of *e.g.* the neutralino mass matrix however can these results be combined to obtain an overall experimental measurement of the spin-dependent scattering cross-section.

The variation of the relative magnitude of $\tilde{\chi}_1^0$-p and $\tilde{\chi}_1^0$-n axial-vector couplings with $\tilde{\chi}_1^0$ composition also leads to some residual model dependency in the shape of the energy spectrum obtained from spin-dependent scattering. The form-factor $S(q)$ relating $\tilde{\chi}_1^0$-nucleus scattering at finite momentum transfer q to that at zero momentum transfer contains terms depending on isoscalar and isovector parameters a_0 and a_1 related to $\tilde{\chi}_1^0$-p and $\tilde{\chi}_1^0$-n coupling parameters a_p and a_n [99]:

$$S(q) = a_0^2 S_{00}(q) + a_1^2 S_{11}(q) + a_0 a_1 S_{01}(q) \tag{2}$$

where

$$a_0 = a_p + a_n, a_1 = a_p - a_n. \tag{3}$$

Here the $S_{ij}(q)$ are independent constituent nuclear form-factors. The differing q dependence of these $S_{ij}(q)$ form-factors means that $S(q)$ differs for differing a_p/a_n and hence differing $\tilde{\chi}_1^0$ composition. This leads to a SUSY model dependency in the shape of the overall energy spectrum. This model-dependency is generally rather small ($\lesssim 10$ % for low energy recoils in e.g. ^{127}I) however the accuracy of direct search measurements of σ_{sd} and $m_{\tilde{\chi}_1^0}$ for comparison with LHC predictions could nevertheless be improved with an estimate from LHC data of the neutralino mass matrix.

7. Conclusions

Recent astrophysical measurements from WMAP and other experiments have strengthened the case for cold dark matter in the universe. Over the next decade the hypothesis of particle cold dark matter will be stringently tested in a number of different ways both with colliders such as the LHC and with non-accelerator experiments such as direct dark matter searches. If SUSY or other BSM physics is discovered at the LHC then measurements of the properties of the new particles particles can be used to predict the properties of dark matter signals in CMB and direct search experiments. Similarly if dark matter is discovered in a direct search experiment model-independent measurements of quantities such as the mass of the dark matter particle can be compared with signals observed at the LHC. Only by combining

these results can we confirm both the existence of non-baryonic cold dark matter and its identity.

Acknowledgments

The work of I.H. and M.B. was supported in part by the Director, Office of Energy Research, Office of High Energy Physics of the U.S. Department of Energy under Contract DE-AC03-76SF00098. Accordingly, the U.S. Government retains a nonexclusive, royalty-free license to publish or reproduce the published form of this contribution, or allow others to do so, for U.S. Government purposes. D.R.T. wishes to acknowledge PPARC for support.

Bibliography

[1] E. L. Wright *et al.*, Astrophys. J. **396** (1992) L13.
[2] D. N. Spergel *et al.*, Astrophys. J. Suppl. **148** (2003) 175 [arXiv:astro-ph/0302209].
[3] C. Alcock *et al.* [MACHO Collaboration], arXiv:astro-ph/9803082;
P. Popowski *et al.*, arXiv:astro-ph/0304464.
[4] R. D. Peccei and H. R. Quinn, Phys. Rev. Lett. **38** (1978) 1440;
S. Weinberg, Phys. Rev. Lett. **40** (1978) 223.
[5] S. J. Asztalos *et al.*, Astrophys. J. **571** (2002) L27 [arXiv:astro-ph/0104200].
[6] M. Davis, F. J. Summers and D. Schlegel, Nature **359** (1992) 393;
G. R. Blumenthal, S. M. Faber, J. R. Primack and M. J. Rees, Nature **311** (1984) 517.
[7] LEPSUSYWG, ALEPH, DELPHI, L3 and OPAL experiments, notes LEPSUSYWG/02-02.1, LEPSUSYWG/01-03.1, note LEPSUSYWG/02-04.1. D. Stewart presented at PHENO 04: Phenomenology 2004 Symposium. April, 2004. University of Wisconsin-Madison Madison.
[8] P. F. Smith and J. R. J. Bennett, Nucl. Phys. B **149** (1979) 525.
[9] L. Alvarez-Gaume, J. Polchinski and M.B. Wise, Nucl. Phys. **B221**, 495 (1983);
L. Iba˜nez, Phys. Lett. **118B**, 73 (1982);
J.Ellis, D.V. Nanopolous and K. Tamvakis, Phys. Lett. **121B**, 123 (1983);
K. Inoue *et al.* Prog. Theor. Phys. **68**, 927 (1982);
A.H. Chamseddine, R. Arnowitt, and P. Nath, Phys. Rev. Lett., **49**, 970 (1982);

For reviews see, H.P. Nilles, Phys. Rep. **111**, 1 (1984);
H.E. Haber and G.L. Kane, Phys. Rep. **117**, 75 (1985).
[10] G. Belanger, F. Boudjema, A. Pukhov and A. Semenov, Comput. Phys. Commun. **149** (2002) 103 [arXiv:hep-ph/0112278].
[11] P. Gondolo, J. Edsjo, P. Ullio, L. Bergstrom, M. Schelke and E. A. Baltz, arXiv:astro-ph/0211238.
[12] B. C. Allanach, S. Kraml and W. Porod, JHEP **0303**, 016 (2003) [arXiv:hep-ph/0302102].
[13] F. E. Paige, S. D. Protopescu, H. Baer and X. Tata, arXiv:hep-ph/0312045.
[14] A. Djouadi, J. L. Kneur and G. Moultaka, arXiv:hep-ph/0211331.
[15] A. Pukhov *et al.*, arXiv:hep-ph/9908288.
[16] J. Edsjo and P. Gondolo, Phys. Rev. D **56**, 1879 (1997) [arXiv:hep-ph/9704361].
[17] G. W. Bennett *et al.* [Muon g-2 Collaboration], Phys. Rev. Lett. **92** (2004) 161802 [arXiv:hep-ex/0401008].
[18] R. Barate *et al.* [ALEPH Collaboration], Phys. Lett. B **565** (2003) 61 [arXiv:hep-ex/0306033].
[19] S. Chen *et al.* [CLEO Collaboration], Phys. Rev. Lett. **87** (2001) 251807 [arXiv:hep-ex/0108032].
[20] M. Carena, H. E. Haber, S. Heinemeyer, W. Hollik, C. E. M. Wagner and G. Weiglein, Nucl. Phys. B **580** (2000) 29 [arXiv:hep-ph/0001002].
[21] J. R. Ellis, K. A. Olive, Y. Santoso and V. C. Spanos, Phys. Lett. B **565** (2003) 176 [arXiv:hep-ph/0303043].
[22] J. L. Feng, K. T. Matchev and T. Moroi, Phys. Rev. Lett. **84** (2000) 2322 [arXiv:hep-ph/9908309];
J. L. Feng, K. T. Matchev and T. Moroi, Phys. Rev. D **61** (2000) 075005 [arXiv:hep-ph/9909334].
[23] J. L. Feng, K. T. Matchev and F. Wilczek, Phys. Rev. D **63** (2001) 045024 [arXiv:astro-ph/0008115].
[24] H. Baer, C. Balazs, A. Belyaev, T. Krupovnickas and X. Tata, JHEP **0306** (2003) 054 [arXiv:hep-ph/0304303].
[25] U. Chattopadhyay, A. Corsetti and P. Nath, Phys. Rev. D **68** (2003) 035005 [arXiv:hep-ph/0303201].
[26] M. Drees and M. M. Nojiri, Phys. Rev. D **47** (1993) 376 [arXiv:hep-ph/9207234];
H. Baer and M. Brhlik, Phys. Rev. D **53** (1996) 597 [arXiv:hep-ph/9508321];
H. Baer and M. Brhlik, Phys. Rev. D **57** (1998) 567 [arXiv:hep-ph/9706509];
H. Baer, M. Brhlik, M. A. Diaz, J. Ferrandis, P. Mercadante, P. Quintana and X. Tata, Phys. Rev. D **63** (2001) 015007 [arXiv:hep-ph/0005027];
A. B. Lahanas, D. V. Nanopoulos and V. C. Spanos, Mod. Phys. Lett. A **16** (2001) 1229 [arXiv:hep-ph/0009065];
J. R. Ellis, T. Falk, G. Ganis, K. A. Olive and M. Srednicki, Phys. Lett. B **510** (2001) 236 [arXiv:hep-ph/0102098].
[27] A. Birkedal-Hansen and B. D. Nelson, Phys. Rev. D **67**, 095006 (2003) [arXiv:hep-ph/0211071].
[28] H. Baer, C. Balazs, A. Belyaev and J. O'Farrill, JCAP **0309** (2003) 007 [arXiv:hep-ph/0305191].
[29] M. Dine, W. Fischler and M. Srednicki, Nucl. Phys. **B189**, 575 (1981);
S. Dimopoulos and S. Raby, Nucl. Phys. **B192,** 353 (1981);
C. Nappi and B. Ovrut, Phys. Lett.**113B,** 175 (1982);
L. Alvarez-Gaumé, M. Claudson and M. Wise, Nucl. Phys. **B207,** 96 (1982);
M. Dine and A. Nelson, Phys. Rev. **D48**, 1227 (1993);
M. Dine, A. Nelson and Y. Shirman, Phys. Rev. **D51,** 1362 (1995);
M. Dine, *et al.*, Phys. Rev. **D53,** 2658 (1996).
[30] G.F. Giudice, R. Rattazzi CERN-TH-97-380, hep-ph/9801271 (1998);
C Kolda, Nucl. Phys. P. Suppl. **62**, 266 (1998).
[31] T. Moroi, H. Murayama and M. Yamaguchi, Phys. Lett. B **303**, 289 (1993).
[32] M. Bolz, A. Brandenburg and W. Buchmuller, Nucl. Phys. B **606**, 518 (2001) [arXiv:hep-ph/0012052].
[33] J. R. Ellis, K. A. Olive, Y. Santoso and V. C. Spanos, Phys. Lett. B **588**, 7 (2004) [arXiv:hep-ph/0312262].
[34] L. Randall and R. Sundrum, Nucl. Phys. B **557** (1999) 79 [arXiv:hep-th/9810155];
G. F. Giudice, M. A. Luty, H. Murayama and R. Rattazzi, JHEP **9812** (1998) 027 [arXiv:hep-ph/9810442].
[35] R. Harnik, H. Murayama and A. Pierce, JHEP **0208**, 034 (2002) [arXiv:hep-ph/0204122];
I. Jack, D. R. T. Jones and R. Wild, Phys. Lett. B **535**, 193 (2002) [arXiv:hep-ph/0202101].
[36] L. E. Ibanez, Phys. Lett. B **137**, 160 (1984).

[37] T. Falk, K. A. Olive and M. Srednicki, Phys. Lett. B **339** (1994) 248 [arXiv:hep-ph/9409270].
[38] M. Mori *et al.*, Phys. Lett. B **289**, 463 (1992).
[39] S. Raby and K. Tobe, Nucl. Phys. B **539** (1999) 3 [arXiv:hep-ph/9807281].
[40] G. D. Coughlan, W. Fischler, E. W. Kolb, S. Raby and G. G. Ross, Phys. Lett. B **131**, 59 (1983); T. Banks, D. B. Kaplan and A. E. Nelson, Phys. Rev. D **49**, 779 (1994) [arXiv:hep-ph/9308292].
[41] T. Asaka, J. Hashiba, M. Kawasaki and T. Yanagida, Phys. Rev. D **58**, 083509 (1998) [arXiv:hep-ph/9711501].
[42] T. Moroi and L. Randall, Nucl. Phys. B **570**, 455 (2000) [arXiv:hep-ph/9906527].
[43] S. Abdullin *et al.* [CMS Collaboration], J. Phys. G **28** (2002) 469 [arXiv:hep-ph/9806366].
[44] ATLAS Collaboration, *ATLAS detector and physics performance Technical Design Report: Supersymmetry*, CERN/LHCC 99-14/15 (1999).
[45] I. Hinchliffe, F.E. Paige, M.D. Shapiro, J. Söderqvist and W. Yao: *Phys. Rev.* **D55** (1997) 5520 9 [ATLAS NOTE ATL-PHYS-97-109].
[46] H. Bachacou, I. Hinchliffe and F.E. Paige: *Phys. Rev.* **D62** (2000) 015009 [ATLAS NOTE ATL-PHYS-2000-010].
[47] B. C. Allanach, C. G. Lester, M. A. Parker and B. R. Webber, JHEP **0009** (2000) 004 [arXiv:hep-ph/0007009].
[48] B. C. Allanach *et al.*, Eur. Phys. J. C **25** (2002) 113 [arXiv:hep-ph/0202233].
[49] G. Polesello and D. R. Tovey, arXiv:hep-ph/0403047.
[50] M. Battaglia, A. De Roeck, J. R. Ellis, F. Gianotti, K. A. Olive and L. Pape, arXiv:hep-ph/0306219.
[51] F. Gianotti, *Precision SUSY Measurements with ATLAS: SUGRA Point 4*, ATLAS NOTE ATL-PHYS-97-110 (1997).
[52] H. Baer, A. Belyaev, T. Krupovnickas and X. Tata, JHEP **0402** (2004) 007 [arXiv:hep-ph/0311351].
[53] H. Baer, C. h. Chen, F. Paige and X. Tata, Phys. Rev. D **53** (1996) 6241 [arXiv:hep-ph/9512383].
[54] S. Asai *et al.*, arXiv:hep-ph/0402254.
[55] ATLAS Collaboration, *ATLAS detector and physics performance Technical Design Report: Heavy Quarks and Leptons*, CERN/LHCC 99-14/15 (1999).
[56] ATLAS Collaboration, *ATLAS detector and physics performance Technical Design Report: Higgs Bosons*, CERN/LHCC 99-14/15 (1999).
[57] I. Hinchliffe and F. E. Paige, in *Proc. of the APS/DPF/DPB Summer Study on the Future of Particle Physics (Snowmass 2001)* ed. N. Graf, eConf **C010630**, E401 (2001).
[58] M. Biglietti *et al.*, *Full Supersymmetry Simulation for ATLAS in DC1*, ATL-PHYS-2004-011 (2004).
[59] I. Hinchliffe and F. E. Paige, Phys. Rev. D **61** (2000) 095011 [arXiv:hep-ph/9907519].
[60] D. Denegri *et al.*, CMS NOTE 2001/032, arXiv:hep-ph/0112045.
[61] T. Appelquist, H. C. Cheng and B. A. Dobrescu, Phys. Rev. D **64** (2001) 035002
[62] H. Georgi, A. K. Grant and G. Hailu, Phys. Lett. B **506**, 207 (2001) [arXiv:hep-ph/0012379].
[63] G. von Gersdorff, N. Irges and M. Quiros, Nucl. Phys. B **635**, 127 (2002) [arXiv:hep-th/0204223].
[64] H. C. Cheng, K. T. Matchev and M. Schmaltz, Phys. Rev. D **66**, 036005 (2002) [arXiv:hep-ph/0204342].
[65] G. Servant and T. M. Tait, Nucl. Phys. B **650**, 391 (2003) [arXiv:hep-ph/0206071].
[66] G. Servant and T. M. Tait, New J. Phys. **4**, 99 (2002) [arXiv:hep-ph/0209262];

[67] H. C. Cheng, K. T. Matchev and M. Schmaltz, Phys. Rev. D **66** (2002) 056006 [arXiv:hep-ph/0205314].
[68] H. C. Cheng, J. L. Feng and K. T. Matchev, Phys. Rev. Lett. **89**, 211301 (2002) [arXiv:hep-ph/0207125];
D. Hooper and G. D. Kribs, Phys. Rev. D **67**, 055003 (2003) [arXiv:hep-ph/0208261];
D. Majumdar, Phys. Rev. D **67**, 095010 (2003) [arXiv:hep-ph/0209277];
G. Bertone, G. Servant and G. Sigl, arXiv:hep-ph/0211342.
[69] K. Agashe and G. Servant, arXiv:hep-ph/0403143.
[70] H. C. Cheng and I. Low, JHEP **0309** (2003) 051 [arXiv:hep-ph/0308199].
[71] A. Birkedal-Hansen and J. G. Wacker, Phys. Rev. D **69** (2004) 065022 [arXiv:hep-ph/0306161].
[72] M. W. Goodman and E. Witten, Phys. Rev. D **31** (1985) 3059.
[73] S. Coutu *et al.*, Astropart. Phys. **11** (1999) 429 [arXiv:astro-ph/9902162].

[74] G. Jungman, M. Kamionkowski and K. Griest, Phys. Rept. **267** (1996) 195 [arXiv:hep-ph/9506380].
[75] M. Drees and M. Nojiri, Phys. Rev. D **48** (1993) 3483 [arXiv:hep-ph/9307208].
[76] J. L. Feng, K. T. Matchev and F. Wilczek, Phys. Lett. B **482** (2000) 388 [arXiv:hep-ph/0004043].
[77] J. R. Ellis, A. Ferstl and K. A. Olive, Phys. Lett. B **481** (2000) 304 [arXiv:hep-ph/0001005].
[78] D. S. Akerib *et al.* [CDMS Collaboration], arXiv:astro-ph/0405033.
[79] R. Bernabei *et al.* [DAMA Collaboration], Phys. Lett. B **450** (1999) 448.
[80] D. Abrams *et al.* [CDMS Collaboration], Phys. Rev. D **66** (2002) 122003 [arXiv:astro-ph/0203500].
[81] A. Benoit *et al.* [EDELWEISS Collaboration], Phys. Lett. B **513** (2001) 15 [arXiv:astro-ph/0106094].
[82] J.C. Barton *et al.* [ZEPLIN1 Collaboration], in *Proc. 4th Int. Workshop on the Identification of Dark Matter*, ed. N.J.C. Spooner and V.A. Kudryavtsev, (World Scientific, 2003).
[83] R. Bernabei *et al.* [DAMA Collaboration], Phys. Lett. B **480** (2000) 23.
[84] R. Bernabei *et al.*, Phys. Lett. B **509** (2001) 197.
[85] U. Chattopadhyay, A. Corsetti and P. Nath, arXiv:hep-ph/0310228.
[86] R. Gaitskell and V. Mandic, *Dark Matter Limit Plotter*, http://cdms.berkeley.edu/limitplots.
[87] B. Ahmed *et al.*, Astropart. Phys. **19** (2003) 691 [arXiv:hep-ex/0301039].
[88] R. Luscher *et al.*, Nucl. Phys. Proc. Suppl. **95** (2001) 233.
[89] T. A. Perera *et al.*, AIP Conf. Proc. **605** (2002) 485.
[90] G. Chardin, arXiv:astro-ph/0306134.
[91] J. Jochum *et al.* [CRESST Collaboration], Phys. Atom. Nucl. **63** (2000) 1242 [Yad. Fiz. **63N7** (2000) 1315] [arXiv:hep-ex/0005003].
[92] R. W. Schnee, D. S. Akerib and R. J. Gaitskell, Nucl. Phys. Proc. Suppl. **124** (2003) 233 [arXiv:astro-ph/0208326].
[93] N. J. Spooner [UKDM and Boulby Collaborations], *Prepared for International Workshop on Technique and Application of Xenon Detectors, Kashiwa, Japan, 3-4 Dec 2001*
[94] D. B. Cline, arXiv:astro-ph/0310439.
[95] E. Aprile *et al.*, arXiv:astro-ph/0207670.
[96] H. V. Klapdor-Kleingrothaus and I. V. Krivosheina, Found. Phys. **33** (2003) 831.
[97] M. J. Carson *et al.*, arXiv:hep-ex/0404042.
[98] D. R. Tovey, R. J. Gaitskell, P. Gondolo, Y. Ramachers and L. Roszkowski, Phys. Lett. B **488** (2000) 17 [arXiv:hep-ph/0005041].
[99] M. T. Ressell and D. J. Dean, Phys. Rev. C **56** (1997) 535 [arXiv:hep-ph/9702290].